AD NUMBER

AD818327

NEW LIMITATION CHANGE

TO

Approved for public release, distribution unlimited

FROM

Distribution authorized to U.S. Gov't. agencies and their contractors; Critical Technology; JUN 1967. Other requests shall be referred to Air Force Institute of Technology, School of Engineering, ATTN: AFIT-SE, Wright-Patterson AFB, OH 45433.

AUTHORITY

AFIT memo dtd 22 Jul 1971

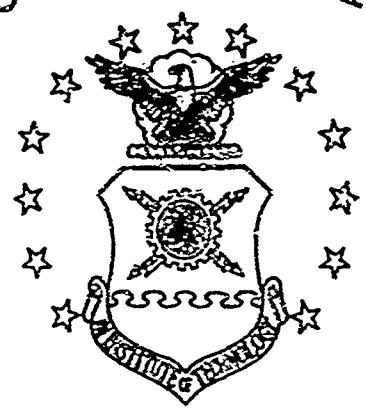

AIR UNIVERSITY
UNITED STATES AIR FORCE

SCHOOL OF ENGINEERING

WRIGHT-PATTERSON AIR FORCE BASE, OHIO

AN INVESTIGATION OF POLARIZATION PHENOMENA PRODUCED BY SPACE OBJECTS

Richard Patton Stead

Lieutenant USAF

GSP/PH/67-7

AFLC-WPAFB-JUL 67 32

GSP/PH/67-7

AN INVESTIGATION OF POLARIZATION PHENOMENA PRODUCED BY SPACE OBJECTS

THESIS

Presented to the Faculty of the School of Engineering

of the Air Force Institute of Technology

Air University

in Partial Fulfillment of the

Requirements for the Degree of

Master of Science

by

Richard Patton Stead

Lieutenant USAF

Graduate Space Physics

June 1967

Preface

The suggestion that this study be undertaken was made by Mr. Kenneth E. Kissell of the General Physics Research Laboratory, Aerospace Research Laboratories. Mr. Kissell has been engaged for a decade in the field of satellite detection and tracking and has taken a major interest in the apparent brightness and color of satellites as a means of cataloging them. Since light is polarized by reflection from a dielectric surface and since some of the surface material on a satellite is dielectric (e.g., solar cells, windows, and glossy paint), it was felt that light reflected from a satellite should show moderate polarization. It is this point that will be investigated in this thesis. Mr. Kissell's guidance, ideas and timely prodding were invaluable to me in working on this thesis.

I wish to express my deep appreciation to Dr. Leno S. Pedrotti, Head of the Physics Department of the Air Force Institute of Technology, for his consent to the undertaking of this investigation as a graduate thesis.

I am deeply indebted to Mr. Richard C. Vanderburgh for his assistance in teaching me the operation of the telescope and the methods involved in satellite prediction and reduction of data.

I would also like to thank Mr. Kenneth Mulvaney for his help in mounting the polarization detector (analyzer) and making it an operational system.

Contents

		Page
Preface		ii
List of Figures		v
List of Tables		vi
Abstract		vii
I.	Introduction	1
	Background	1
	Scope of Study	2
II.	Theory	4
	Reflectivity of a Surface	4
	Polarization by Reflection	6
	Polarization Percentage	7
	Reflected Light Equations	7
	Surface Characteristics of Space Objects	7
	Geometry of a Space Object	8
	Orientation in Space	11
	Illumination of a Space Object	11
	Earth-Space Object Geometry	11
	Specularly Reflecting Sphere	15
	Specularly Reflecting Cylinder	16
	Determination of the Plane of Polarization	18
III.	Equipment	24
	Basic Overall System	24
	Photoelectric Photometer	24
	Tape Recorder	24
	Oscillograph	26
	Four-Axis Mount	26
	Polarization Analyzer	29
IV.	Collection of Data	34
V.	Analysis of Data	37
	Space Object #893	37
	Percent Polarization	37
	Error Removal from Percent Polarization	40
	Variation of the Percent Polarization with the Phase Angle	42
	Absolute Magnitude of a Space Object	43

Probable Value for the Index of Refraction 45
Plane of Polarization 48
Comparison with an Unpolarized Record 50
Probable Explanation for Peaks 51
Space Object #1092 51
Comparison with an Unpolarized Record 51
Explanation for No Apparent Polarization 54

VI. Conclusions and Recommendations 55

Conclusions 55
Recommendations 55

Bibliography 57

Appendix A: Four-Axis Geometry 58

Appendix B: Sample calculation. 60

Vita 62

List of Figures

Figure		Page
1	Dielectric Reflecting Surface	5
2	Effect of a Curved Surface on the Polarizing Angle	9
3	Earth-Space Object Geometry	13
4	Specularly Reflecting Sphere	14
5	Specularly Reflecting Cylinder	17
6	Telescope Mount Referenced to the Celestial Sphere	20
7	Spectral Response Curve for the RCA 7029 Photomultiplier	25
8	The ARL 24-Inch Telescope	27
9	Illustration of the Mounting Nomenclature and Symbols	28
10	Polarization Analyzer	30
11	Schematic Representation of the Analyzer	31
12	Photometric Recordings of Space Object #893	38
13	Calibration Curve for 21 November 1966	39
14	Percent Polarization versus Angle of Incidence	46
15	Photometric Recording of Space Object #426	49
16	Ablestar Rocket Body	52
17	Photometric Recordings of Space Object #1092	53
18	Celestial Sphere Representation of Local Satellite Trajectory	59

List of Tables

Table		Page
I	Peak Polarisation Percentages	40
II	Corrected Peak Polarisation Percentages	42
III	Polarisation Dependence on Phase Angle	43
IV	Absolute Magnitudes of the Peaks	44
V	Polarizing Angles for Glossy Paints	48

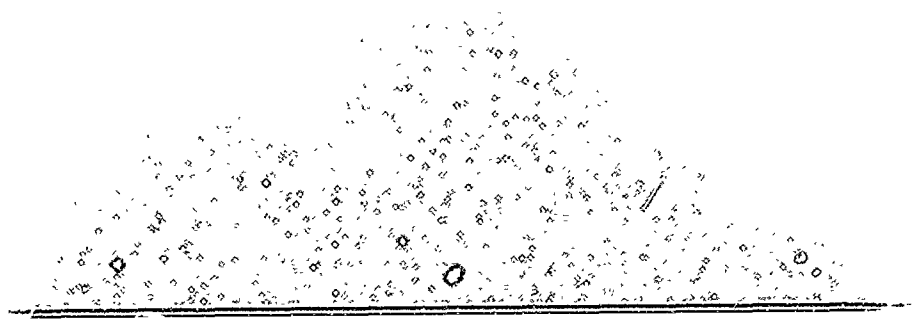

Abstract

Plane polarized light produced by the reflection of sunlight from a dielectric surface on a space object was observed. This was accomplished with a polarization analyzer which was added to the existing photoelectric telescope and recording equipment at the Sulphur Grove, Ohio tracking station. A maximum of 39% polarization was measured for one particular satellite (Space Object #893). The plane of polarization was found to be perpendicular to the plane of incidence as expected.

GSP/PH/67-7

AN INVESTIGATION OF POLARIZATION PHENOMENA PRODUCED BY SPACE OBJECTS

I. Introduction

Since the first results from research conducted by the United States Air Force Avionics and Aerospace Research Laboratories indicated that the temporal variations of the integrated light received from a space object contained detailed information on the surface characteristics, surface finish, and dynamical motions of the object, signature data have been collected from over approximately 150 orbiting objects at slant ranges from 125 to 5000 statute miles. Analysis of these data has enabled the classification of objects by similarities in overall signature patterns, by surface finish (specular, diffuse paint, or glossy paint), and by surface protuberances. Up to this present work no attempt had been made to detect polarization effects in the light scattered by a space object and to use such effects as another identifying property in an overall classification system. In order to detect polarized light, however, the problem of separating the polarized portion of the reflected light from the unpolarized portion had to be solved.

Background

Even before the launching of the first earth satellite, the optical characteristics of a specular reflecting and a diffuse reflecting spherical satellite were predicted (Ref 14:24-25). However, the observation of space objects by optical means is largely restricted to the location and cataloging of space objects by position in

space. Only minor concern is given to the apparent brightness and color of a space object, and no concern at all has been given to any of the polarization qualities a space object may have. Indeed, according to Kissell (Ref 7:74):

> ....prior efforts include attempts to determine the range of fluctuations and times of maximum brightness with intention to relate these to orientation, to use photoelectric measurements for study of selective and broad-band absorption of sunlight in the upper atmosphere, and to deduce orientation of space objects specially equipped with mirrors to produce specular flashes. More recently work has been directed at the surface properties of the space objects in terms of secular effects on surface finishes.

The present telescope system at the ARL tracking station on a dark, transparent night, is capable of yielding measurable records above the system noise for space objects of +11 stellar magnitudes, i.e., 1/100 of the threshold of naked eye sensitivity (Ref 7:75). However, for polarization measurements the sensitivity is somewhat reduced (+7 stellar magnitudes) due to the absorption introduced by the addition of the polarization analyzer to the system. Nevertheless, it is important to understand that the system is quite capable, on a regular operational basis, of obtaining a nearly continuous track of the various types of objects usually put into orbit.

Scope of Study

Theoretical polarization predictions for sunlight reflected from space objects were to be made based on certain mathematical models. These were to be compared with the experimental results which represented actual space objects. Also, inference of surface characteristics from the polarization measurements were to be considered. The

purpose, therefore, was to make theoretical polarization predictions based on certain mathematical models and from these predictions devise an experimental method that would enable the detection and measurement of the expected polarization effects.

Photoelectric polarization measurements of reflected sunlight from some United States and Russian space objects of known and unknown surface characteristics were to be made and interpreted. The observations were to be performed with the existing tracking and recording equipment located at the Sulphur Grove, Ohio tracking station of the Aerospace Research Laboratories with the addition of an analyzer to be designed by the author.

It should be mentioned that it was not possible to obtain polarization measurements of the space objects actually observed before they were put into orbit. In addition, the effect of the space environment on their surfaces between launch and observation is an unknown. Also, a detailed analysis of the dynamical motions of the objects was not made, i.e., the exact orientation of the objects in space at the time of observation was unknown.

II. Theory

Polarization of light by reflection and the percentage of such polarization will be discussed. The effect of different indexes of refraction on the intensity and on the percent polarization of the reflected light will likewise be discussed. Also, the factors of primary importance in determining the illuminance received by an observer from a given model of a space object will be discussed and the illuminance equations presented and related to the conditions necessary for observing polarization.

Reflectivity of a Surface (Ref 4:29)

The reflectivity of a plane, dielectric surface is the fraction of incident light that is reflected. It can be determined from the Fresnel equations, (reference Figure 1)

$$\frac{I_\perp}{I_{o\perp}} = \frac{\sin^2 (i-r)}{\sin^2 (i+r)} \qquad (1)$$

$$\frac{I_{||}}{I_{o||}} = \frac{\tan^2 (i-r)}{\tan^2 (i+r)} \qquad (2)$$

where I_o and I are the incident and reflected intensities respectively and where the subscripts $\perp$ and $||$ denote the perpendicular and parallel components of the electric vector of the light as referenced to the plane of incidence (i.e., plane of the paper). The light which is not reflected is transmitted by the dielectric since it is assumed that the dielectric does not absorb.

Natural or unpolarized light may be assumed to consist of equal amounts of two components that are plane polarized perpendicular to

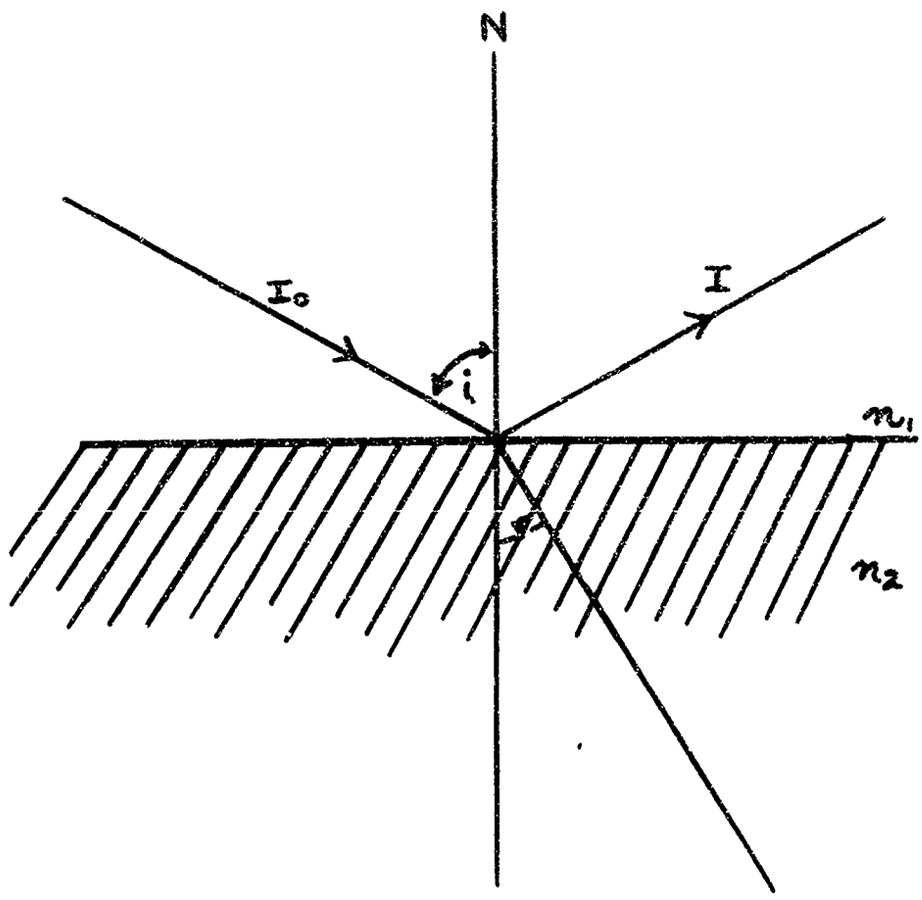

Fig. 1

Dielectric Reflecting Surface

each other i.e., $I_{o\perp} = \frac{1}{2}(I_o)$ and $I_{o\parallel} = \frac{1}{2}(I_o)$. Thus the amount of natural light that is reflected at the surface between two transparent media can be obtained in the following way:

$$I = I_\perp + I_\parallel \tag{3}$$

$$\frac{I}{I_o} = \frac{I_\perp}{I_o} + \frac{I_\parallel}{I_o} \tag{4}$$

$$\frac{I}{I_o} = \frac{I_\perp}{2I_{o\perp}} + \frac{I_\parallel}{2I_{o\parallel}} \tag{5}$$

Substituting Eqs. (1) and (2) in the above equation gives

$$\frac{I}{I_o} = \frac{\sin^2(i-r)}{2\sin^2(i+r)} + \frac{\tan^2(i-r)}{2\tan^2(i+r)} \tag{6}$$

Polarization by Reflection

In Eq. (6) it can be seen that if natural light is incident on the surface at an angle such that $i + r = 90°$, the second term becomes zero and the reflected light is said to be completely plane polarized in the plane of incidence. This means that the reflected light contains only that component of the electric vector which is perpendicular to the plane of incidence, as defined by the first term of Eq. (6).

The law of refraction is given by Snell's equation

$$\frac{\sin i}{\sin r} = n_2/n_1 = n_{12} \tag{7}$$

Since $i + r = 90°$, $r = 90° - i$. Therefore Eq. (7) becomes

$$\frac{\sin i}{\cos i} = n_{12}$$

or

$$\tan i_p = n_{12} \tag{8}$$

where i_b is the polarizing or Brewster angle. All light reflected at this angle is one hundred percent plane polarized.

Polarization Percentage (Ref 5:231)

The percent polarization is defined by the equation

$$\% \text{ polarization} = \frac{I_{max} - I_{min}}{I_{max} + I_{min}} \times 100 \qquad (9)$$

where I_{max} and I_{min} are the maximum and minimum intensities respectively. When a polarizing analyzer is introduced into a partially polarized beam, I_{max} and I_{min} represent the extremes of intensity as the analyzer is rotated. I_{min} will occur when the analyzer is oriented such that a specified reference vector on the analyzer is parallel or antiparallel to the plane of vibration of the electric vector. In the case of reflection as in Figure 1, the specified reference vector will be defined to be parallel to the reflecting surface at minimum transmission of light reflected from the surface. Thus at maximum light, the specified reference vector will be contained in the plane of incidence.

Reflected Light Equations

The amount of sunlight reflected by an object in space depends upon its surface characteristics, its size and shape, and upon the orientation and position of the object.

Surface Characteristics of Space Objects. Since the surface of space objects may be composed of many types of metals, paints, and

other materials, the type of light reflection will be unknown. A polished metal surface will give a specular type of reflection as will a window, solar cell, or glossy paint while a non-glossy paint or matte surface will reflect diffusely. Polished metal, non-glossy paint, and matte surfaces should show no signs of linear polarization because they are either non-dielectric or light scattering surfaces. Just the opposite is true for a window, solar cell, or glossy paint since they are specular reflectors and dielectric. For this case Eq. (8) is applicable and linearly polarized light should be detectable. The illumination received from most space objects however, will be of combined origin i.e., be produced by both diffuse and specular processes from different parts of the spacecraft. Separate equations will be presented for each type of scattering process.

Geometry of a Space Object. Shapes and sizes of space objects vary considerably and can exhibit many irregularities. However, they are important because the area of a space object illuminated by the sun, and thus the amount of light reflected toward the observer, depends upon the geometrical size and shape. For this investigation only spheres and cylinders will be considered for the mathematical models in order to simplify the derivations. However, it should be mentioned that these two forms are represented in a large number, if not the majority, of the objects of interest.

The size and shape of a space object have no real effect on the polarization properties, just on the energy available for detection. The larger the area of a specular, dielectric surface the higher the intensity of observed polarized light. Therefore, the larger the sur-

face the easier it is to detect polarization. For the 24-inch telescope system used in this investigation the minimum brightness for detecting polarization would be approximately +3 to +7 magnitudes, or 6×10^{-11} to 1.5×10^{-12} watts (Ref 7:83). Below this level sky background and equipment noise interfere with the signal and make the detection of any polarization difficult. However, specular reflections from the objects observed in this study (depending upon their orientation and distance from the observer) will almost always fall in or above this range. For example, consider the case of a flat mirror at a distance of 1000 km from an observer. What size would the mirror have to be in order for the observer to detect a brightness of +5 stellar magnitudes?

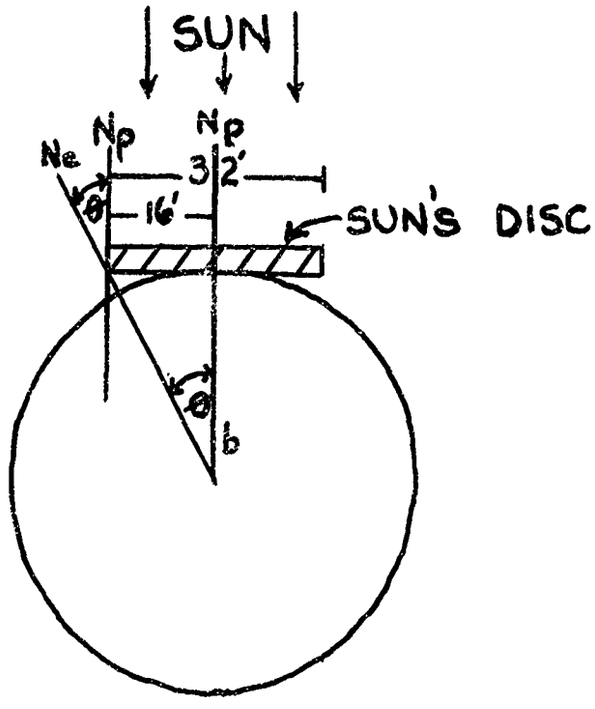

Fig. 2

Effect of a Curved Surface on the Polarizing Angle

Assuming that the reflectivity of the mirror is 1.00, that any absorption due to the atmosphere has been removed by a calibration process, that the observer is within the ½ degree cone subtended by the sun's image in the mirror, and that the cone has an angle of incidence with the earth of approximately 60°; the area of the mirror would be 0.02 in^2. See Appendix B for the calculation.

Also, it will be remembered that in the steps leading up to the derivation of Eq. (8), the light was assumed to be incident on a plane surface. How well this plane surface approximates the curved surfaces of the spherical and cylindrical models will now be investigated.

In Figure 2, N_p and N_c are the surface normals to the tangent plane and the curved surface (sphere or cylinder) respectively. The radius is b. The angle θ is measured from the point of tangency where N_p and N_c are the same to the edge of the disc formed by the image of the sun in the tangent plane. It represents the maximum error involved in measuring the angle of incidence from the normal to the plane rather than from the normal to the curved surface. The quantity of interest, therefore, is the angle between the normal to the plane and the normal to the curved surface which is also θ. Since the angular diameter of the sun at the earth is essentially a constant (32 minutes of arc), the maximum angle θ between N_p and N_c is also a constant.

From Figure 2 this constant maximum angle θ is given by $\tan^{-1}$ (16'/b). Using a unit radius and the fact that for small angles the tangent of an angle is equal to the angle itself, θ is equal to 16

minutes of arc. This is certainly negligible when considering polarizing angles.

Orientation in Space. Knowledge of the orientation of a space object, while important in determining whether light striking a particular surface of the object can be seen by an observer on the earth, is not essential in order to anticipate polarization effects. In fact, from experience it is known that for any given transit certain objects exhibit specular flashes which, if they are caused by dielectric surfaces (i.e., solar cells, sapphire window, or glossy paint), should be highly plane polarized. Moreover, an object tumbling across the sky scattering sunlight to an observer allows the observer to sample light reflected from numerous parts on its surface, no matter how they are attached or oriented on the object.

Illumination of a Space Object. Since the distance from the sun to a space object in the vicinity of the earth is essentially constant for any given transit, the luminous flux received from the sun is also essentially a constant. This constant is taken to be 13,136 lumens/feet^2 (Ref 1:138). Any other light arriving at the space object from other sources, such as the earth or moon, will be considered negligible (Ref 9:5).

Earth-Space Object Geometry. If a plane surface (such as the one in Figure 1) were put into orbit around the earth, polarized light would be observed provided the light was incident around the polarizing angle and that the observer was in the path of the reflected light. This last point is of particular interest in this case

since the beam from a flat mirror is highly directional. The beam forms a solid angle of 32 minutes of arc. This is due to the fact that the sun (and its image in the plane mirror) subtends an angle of 32 minutes. Therefore, the brightness of the mirror surface is the brightness of the sun only if observed within this small ½° cone. Outside this cone the brightness is zero. The illumination E received by an observer from a plane surface object is given by

$$E = \frac{I\omega}{A} \tag{10}$$

where E = illumination (lumens/ft^2)

A = area illuminated (ft^2)

I = luminous intensity of object (lumens/solid angle)

ω = solid angle substended by the area A

$I\omega$ = luminous flux (lumens)

From Figure 3 it can be seen that for a plane surface, which can be represented mathematically by a normal to its surface, the angle of incidence is equal to the angle of reflection (provided, of course, the surface is specular). Therefore, unless the plane is tumbling as it goes across the sky, the observation of the plane will be a one time event occurring when the angle of incidence is such as to cause the reflected beam to intercept the earth at the observer's position. A person located at point X in Figure 3 would not be able to see the plane at the same time as a person at the point designated as observer. Instead, he would have to wait until the plane moved along its orbit to a point where the reflected light cone intercepts the observer's position on the earth.

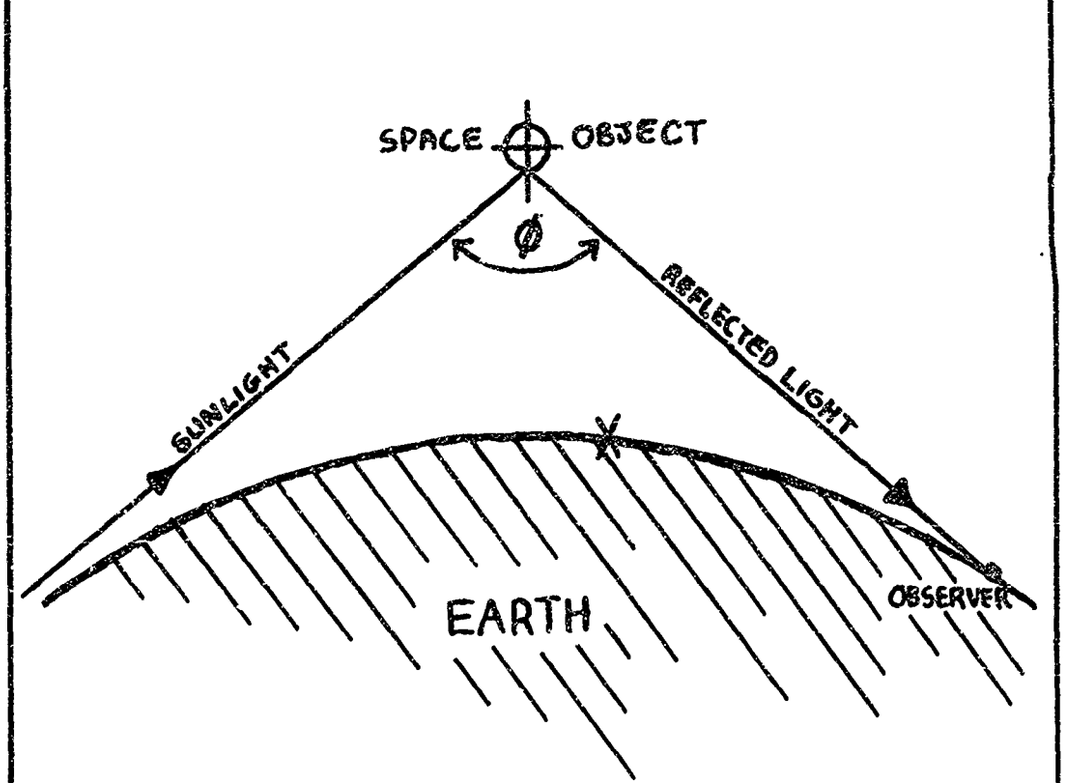

Fig. 3

Earth-Space Object Geometry

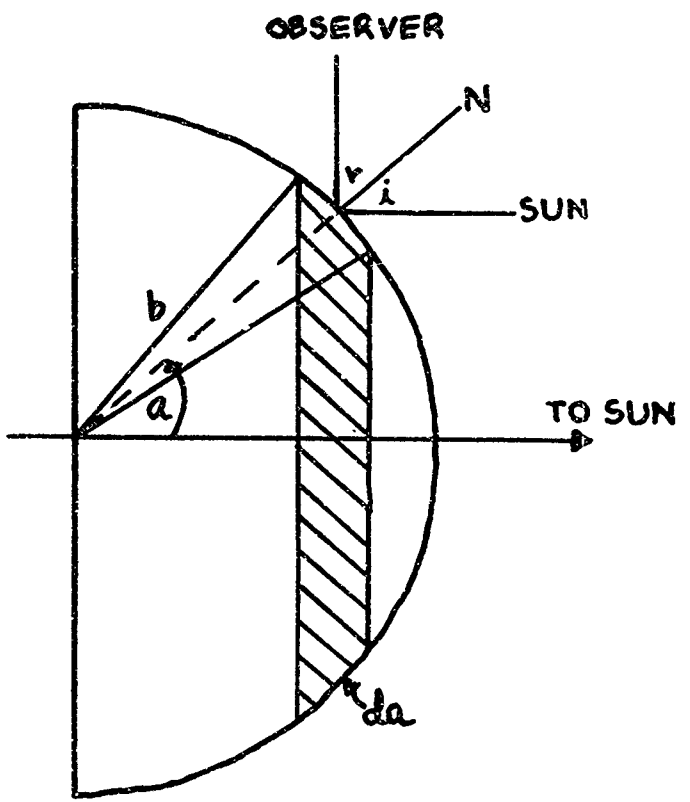

a. During Reflection

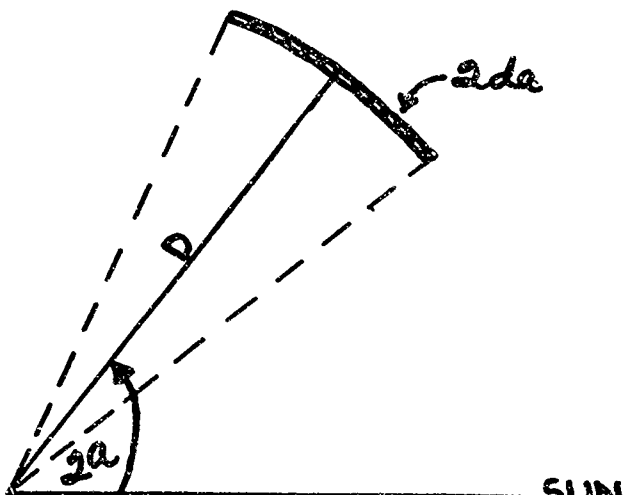

b. After Reflection

Fig. 4

Specularly Reflecting Sphere

For the Sulphur Grove, Ohio tracking station the maximum practical value which the phase angle $\emptyset$ can attain is about 140°. This would occur when the object is slightly above the horizon where the sun has just set or is just about to rise. This means that the maximum which the reflected polarizing angle can have is 70°. This corresponds, from Eq.(8), to an index of refraction of 2.75. However, it should be noted that this only represents the maximum value of refractive index at which 100% polarization can occur. It is still possible to obtain partially polarized light from surfaces of higher indexes of refraction for incidence angles of less than 70°. Several substances have indexes of refraction for 100% polarization, which correspond to angles of 60° or less. These include glass (56°) and glossy paints (60°).

Specularly Reflecting Sphere (Ref 12:24-25). The light reflection equations for the various mathematical models mentioned earlier can now be presented. In order to derive the observed illuminance for the specular reflector let $2a = \emptyset$ as previously defined. This implies specular reflection since the angle of incidence must equal the angle of reflection or if $i = r = a$, then $i + r = 2a$. Consider the radiation incident on a spherical zone whose angular radius is "a" and whose width is da as shown in Figure 4(a). The area of the zone da is just $2\pi b \sin a \times b\, da$. Also, the amount of incident flux a surface element receives is dependent upon the projected area seen by the sun, i.e., proportional to cos a. Therefore the luminous flux incident on the zone is given by

$$dF = E_0\, 2\pi b^2 \sin a \cos a\, da \qquad (11)$$

where E_o is the illuminance at the sphere due to the sun, and b is the radius. After reflection at a distance D from the sphere this flux falls on an area dA of $2\pi D \sin 2a \times D(2da)$. The 2a and 2da terms are present because after reflection from the surface the incident ray has undergone a change of direction equal to i + r or $\emptyset$ which is equal to 2a (see Figure 4(b)). The observed illuminance is then

$$E = \frac{dF}{dA} = \frac{2\pi b^2 E_o \sin a \cos a \, da}{2\pi D^2 \sin 2a \, (2da)} = \frac{b^2 E_o}{4D^2} \qquad (12)$$

Note that the observed illuminance for the specular sphere is independent of "a". The specular sphere is a very favorable reflector. The polarization properties of a specular sphere are dependent strictly upon the reflecting material and the phase angle. A dielectric, specular sphere would therefore be an excellent object for polarization studies.

Specularly Reflecting Cylinder (Ref 3:119). In order to derive the equation for the amount of illuminance received by an observer from a specularly reflecting cylinder, consider the diagrams in Figure 5. The light is incident on a strip of length h and width b $d\theta$. The amount of incident flux received by a surface element is proportional to cos a. Therefore the luminous flux incident on the strip is given by

$$dF = E_o \, hb \cos a \cos \frac{\theta}{2} \, d\theta \qquad (13)$$

After reflection at a distance D from the cylinder, this flux falls on an area of $hD \cos a \, (2d\theta)$. The $2d\theta$ is present because

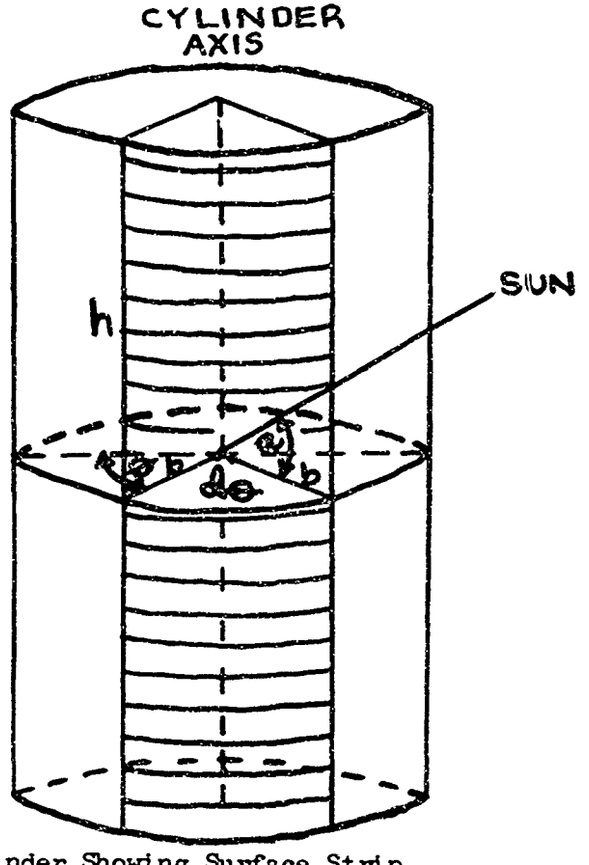

a. Cylinder Showing Surface Strip

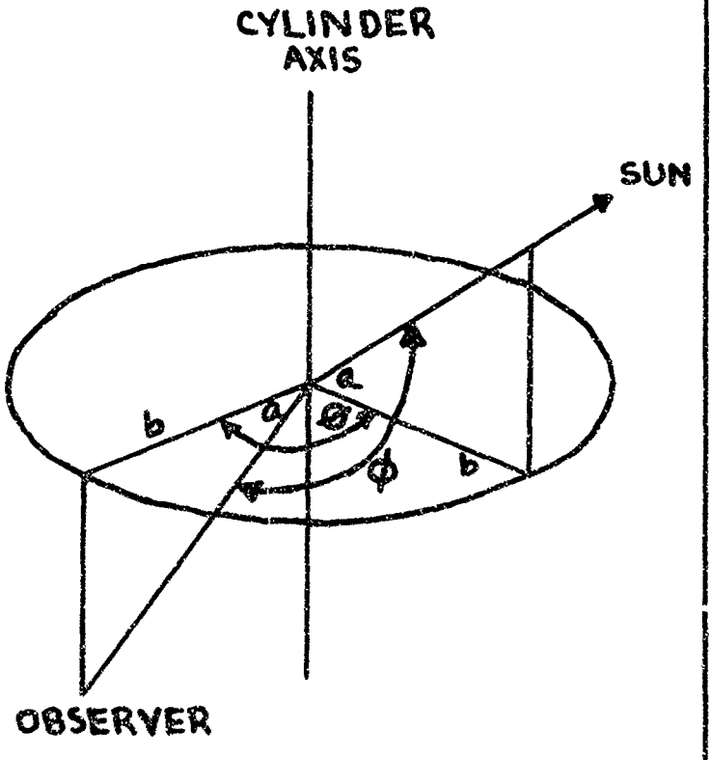

b. Cylinder Showing Important Angles

Fig. 5 Specularly Reflecting Cylinder

the incident rays undergo a change of direction equal to $2d\theta$ upon reflection from the surface (similar to the situation shown in Figure 4(b)). Therefore, the observed illumination is

$$E = \frac{dF}{dA} = \frac{E_0 \, hb \cos \theta/2 \cos a \, d\theta}{2hD \cos a \, d\theta} \tag{14}$$

or, since $\cos a \cos \theta/2 = \cos \phi/2$ (where ϕ is the phase angle)

$$E = \frac{E_0 \, b \cos \phi/2}{2D \cos a} \tag{15}$$

Note that the illuminance received by an observer is dependent on the phase angle. If the surface has some dielectric material on it, one would again expect to be able to observe linear polarization for a polarizing angle near half the phase angle value. Therefore, a specular cylinder is a good object for polarization measurements.

It should be mentioned that in the equations developed so far allowance has to be made for atmospheric absorption. Also, only specular reflectors have been considered in the derivations. Diffusely reflecting objects are of no interest as far as observing polarization is concerned because any light reflected from a diffuse surface will be randomly scattered. Therefore, even if the light were polarized before reflection, it would not be detectable as polarized light after reflection from such a surface. However in actuality, most space objects are a combination of diffuse and specular reflectors.

Determination of the Plane of Polarization. There is one final point which should be investigated concerning the nature of polarized light. One would like to know how the plane of polarization of the

reflected light is oriented. The orientation is determined from the definitions discussed earlier on page 7. For a specular flash from a space object the plane of incidence is the plane containing the sun, space object, and observer. From Figure 1 it can be seen that if the electric vector is vibrating in the plane of incidence (i.e., in the plane of the paper) and the refracted and reflected ray are 90° apart (condition for polarizing angle), there can be no reflected ray. This is true because the electric vector of the reflected ray would then be vibrating in such a way as to be parallel to the direction of propagation of the reflected ray. This is a physical impossibility since light is a transverse wave with its components vibrating perpendicular to the direction of propagation. However, there is an allowed reflected ray for the electric vector vibrating perpendicular to the plane of incidence. In the case of a space object this plane is continually changing due to the motion of the space object across the sky. The orientation is best determined by referencing the plane of incidence to the telescope and taking the electric vector as being perpendicular to this plane. This can be done by using either an analogue technique or by a direct analytical solution. The latter will now be considered, although in practice the former is easier if one is not using a computer program. Consider the positions of the space object and observer on the celestial sphere as illustrated in Figure 6.

In Figure 6 the observer is at the center of the celestial sphere and his zenith, the point directly overhead, is Z. His horizon is 90° away from Z and is represented by the horizontal plane through the sphere. S is the position of the space object on the celestial

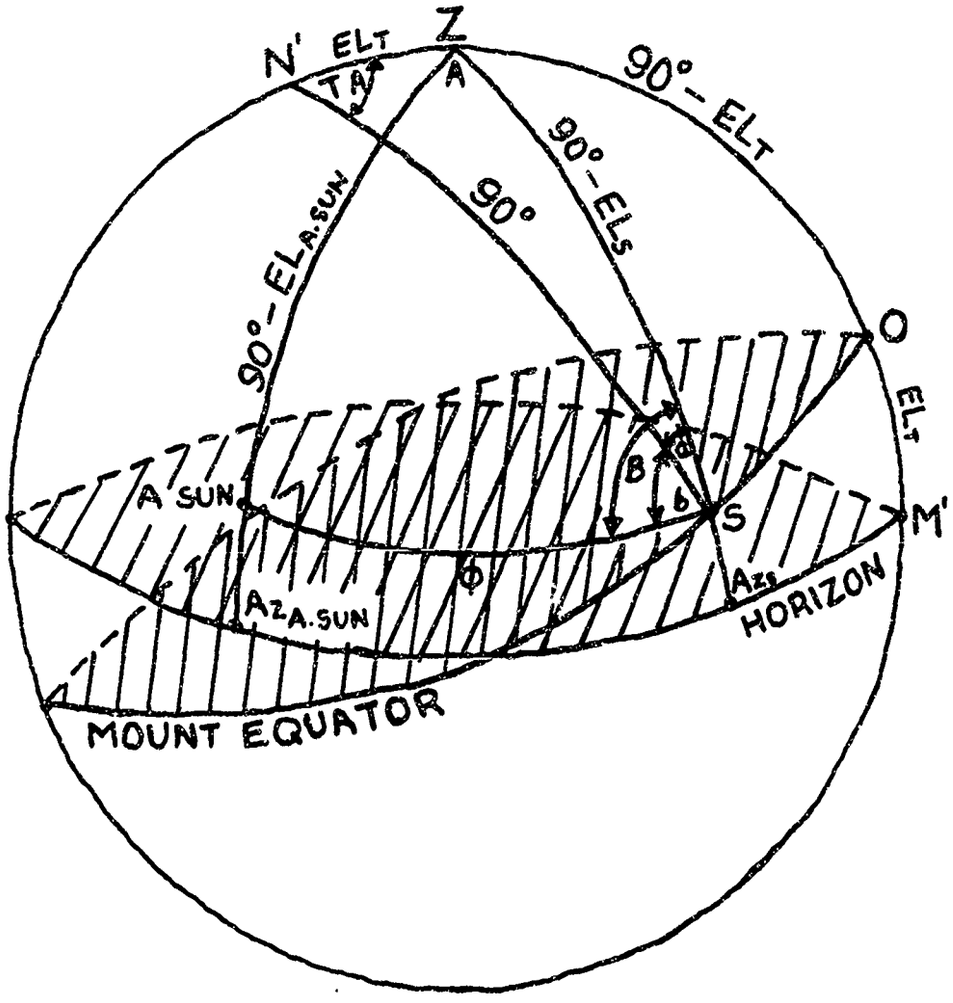

Fig. 6

Telescope Mount Referenced to the Celestial Sphere

sphere at the time of interest. ASun is the position of the antipodal sun, diametrically opposite the true sun on the celestial sphere. The antipodal sun is used to make the spherical triangles easier to handle. N′ is the telescope's pole position, and 90° away is the telescope, or mount, equator along which the space object is moving. It should be noticed from the four-axis geometry in the appendix that one of the four axes, declination, was set to zero for the illustration in Figure 6. The introduction of the declination in the problem will in no way affect the validity of the equations which will be developed, just the value of some of the angles (TA and EL_t) which are substituted in these equations. The point designated 0 is the midpoint of the space object's path across the observer's sky. It is also the point which determines the elevation setting, EL_t, for the telescope mount. M′ is the azimuth setting of the mount for this point. TA is the track angle of the space object, which is the angular distance along the orbit as measured at the telescope. The angle A is the difference in azimuth between ASun and S, and $\emptyset$ is the phase angle.

First of all, in order to determine anything about the orientation of the plane of polarization it is necessary to know how the analyzer which detects the polarization is oriented with respect to the mount. The analyzer is put on the mount so as to be at an angle of 45° from the mount meridian, which is represented by the arc N′S in Figure 6. If a vertical circle is drawn through S (arc ZS), it is possible to determine another angle "a" which represents the angular displacement of the mount meridian from the vertical. The angle "a" may be computed by using the law of sines for a spherical triangle.

$$\frac{\sin TA}{\sin ZS} = \frac{\sin a}{\sin EL_t}$$

or
$$\sin a = \frac{(\sin TA)(\sin EL_t)}{\sin (90 - EL_s)} \tag{16}$$

where EL_t and EL_s are the mount elevation setting and space object elevation respectively. Everything except "a" is known either from orbital predictions or direct reading of the mount settings. Therefore, "a" can be uniquely determined.

If the sun's position on the celestial sphere is now considered, the phase plane (common plane for sun, space object, and observer) is defined. This phase plane will then intercept the mount meridian N'S at some angle b. This angle may be computed from triangle ZASunS by using the law of sines to determine B and noting that $b = B \pm a$. The plus sign is used if B is less than or equal to "a" and the minus if B is greater than "a" as illustrated in Figure 6. This convention will enable the determination of b no matter which side of the vertical circle ZS the mount meridian N'S is located. Since "a" has already been computed, b follows immediately once B has been determined.

$$\frac{\sin B}{\sin ZASun} = \frac{\sin A}{\sin \phi}$$

or
$$\sin B = \frac{(\sin A)(\sin 90 - EL_{asun})}{\sin \phi} \tag{17}$$

where EL_{asun} is the local elevation of the antipodal sun, and the other quantities are as defined above.

With the angles 45° (angle between mount meridian and reference signal for vertically polarized light) and b now determined, the orientation of the electric vector with respect to the mount meridian is

uniquely defined. This assumes the electric vector to be vibrating perpendicular to the phase plane.

III. Equipment (Ref 7:75)

Basic Overall System

The equipment used to make photometric recordings at the Sulphur Grove site consists of a 24-inch Cassegrain optical system of 384 inch focal length attached to a special tracking mount which provides the ability to approximate motion of a satellite to within one arc minute. Light is focused on a photomultiplier and the multiplier output is recorded on an FM tape recorder. Voltage is simultaneously applied to a Honeywell Visicorder for visual representation along with the time signal from WWV and a position reference marker derived from the polarization analyzer as described below.

Photoelectric Photometer

The photomultiplier used was an RCA 10-stage, domer-window type 7029 with extremely high cathode sensitivity. The secondary-emitting dynodes are especially suited for use under high ambient light levels. Its spectral response peaks at 5000 A. Figure 7 is a plot of the spectral response for the photomultiplier with and without the HN-32 sheet Polaroid analyzer. The photomultiplier is energized by a Sweet-type logarithmic feedback power supply which maintains a constant output current from the photomultiplier by regulating the dynode voltage. This gives a roughly linear response in stellar magnitudes over a range of 10 to 15 magnitudes and effectively prevents overloading of the photomultiplier by accidental overexposure.

Tape Recorder

For permanent recordings and versatile playback of data a fre-

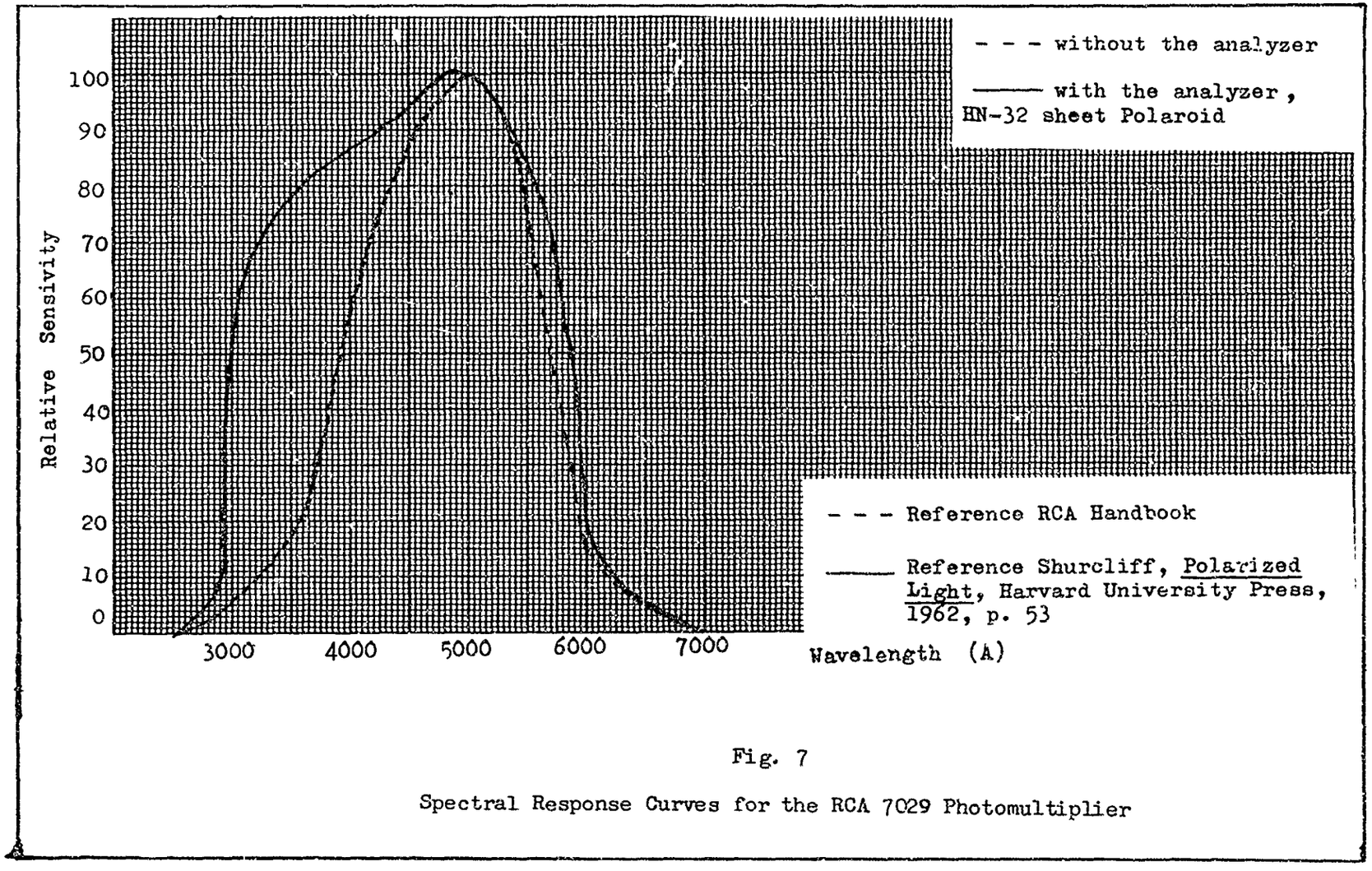

Fig. 7

Spectral Response Curves for the RCA 7029 Photomultiplier

quency-modulated Ampex tape recorder is used, type SP-300.

Oscillograph

In order to have a real time output the signal from the photometer is fed directly into a Honeywell Model 1508 Visicorder. The output from the Visicorder is on Direct-print Linograph paper made by the Eastman Kodak Company.

Four-Axis-Mount (see Figure 8)

The mount was originally a three-axis system but was later modified by Kissell and Nunn to allow for the four-axis mounting of an f/16 24-inch Cassegrain telescope, along with a viewfinder.

A 13 x 125 elbow finder scope was designed to provide two turreted eyepieces with 1° and 6° fields of view and to be attached in a parallelogram arrangement with the telescope. The arrangement minimizes eyepiece movement with changes in telescope position. Precision bearings for the parallelogram movement and a rigid structure for the finder mounting were used to keep the optical axes of the finder and the telescope in close coincidence over the range of motion of the tracking axes. The active field of the photometer could be checked on each observing run by boresighting on any convenient star.

Symbols for each of the four axes, and the component nomenclature, are shown in Figure 9 (see the appendix for a discussion of the four-axis geometry). The motions of the telescope as described by Vanderburgh (Ref 12:2-5) will now be presented.

> Motion about the A axis is accomplished by manual turning of the main yoke. Electrical drive is unnecessary,

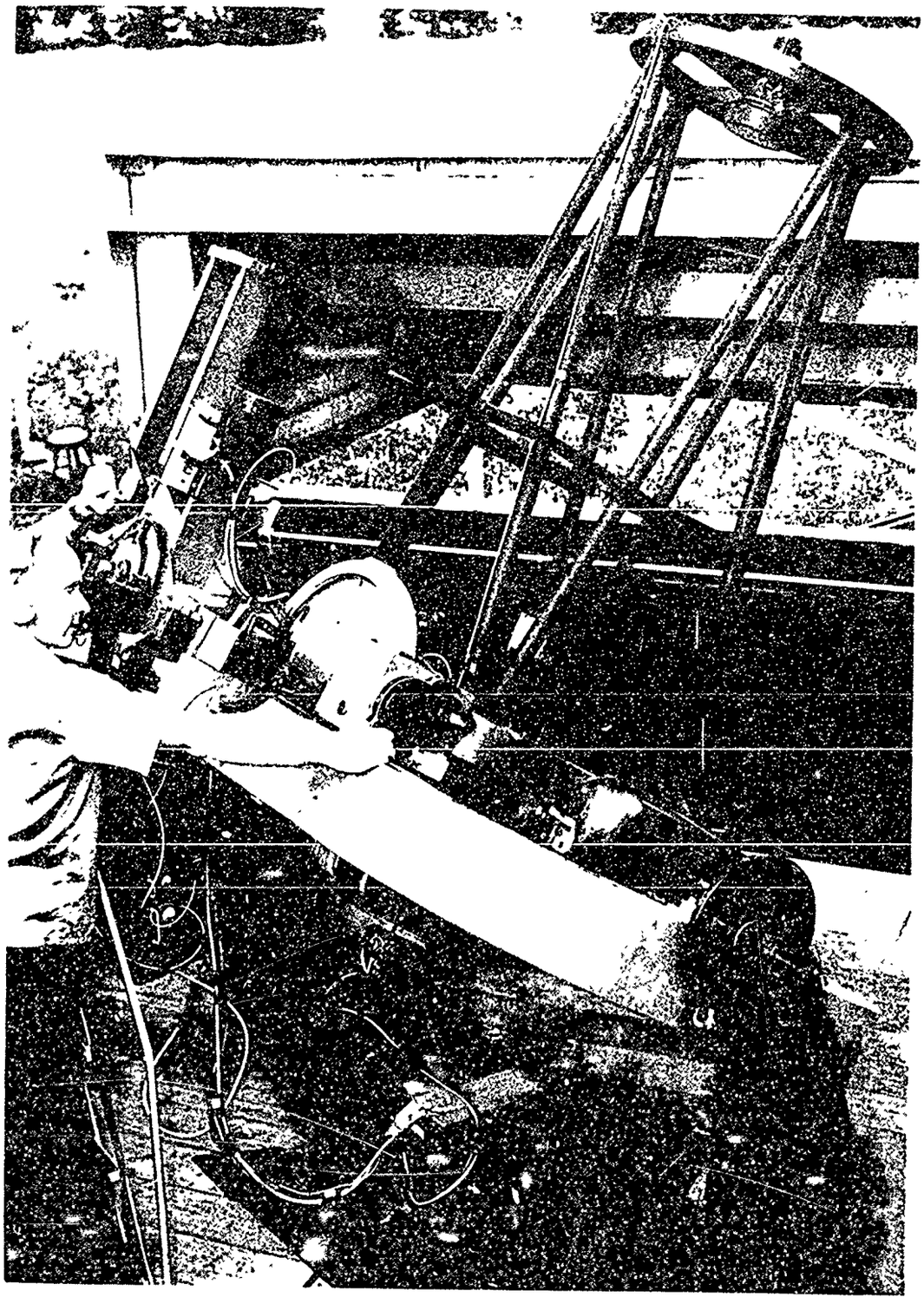

Fig. 8

The ARL 24-Inch Telescope

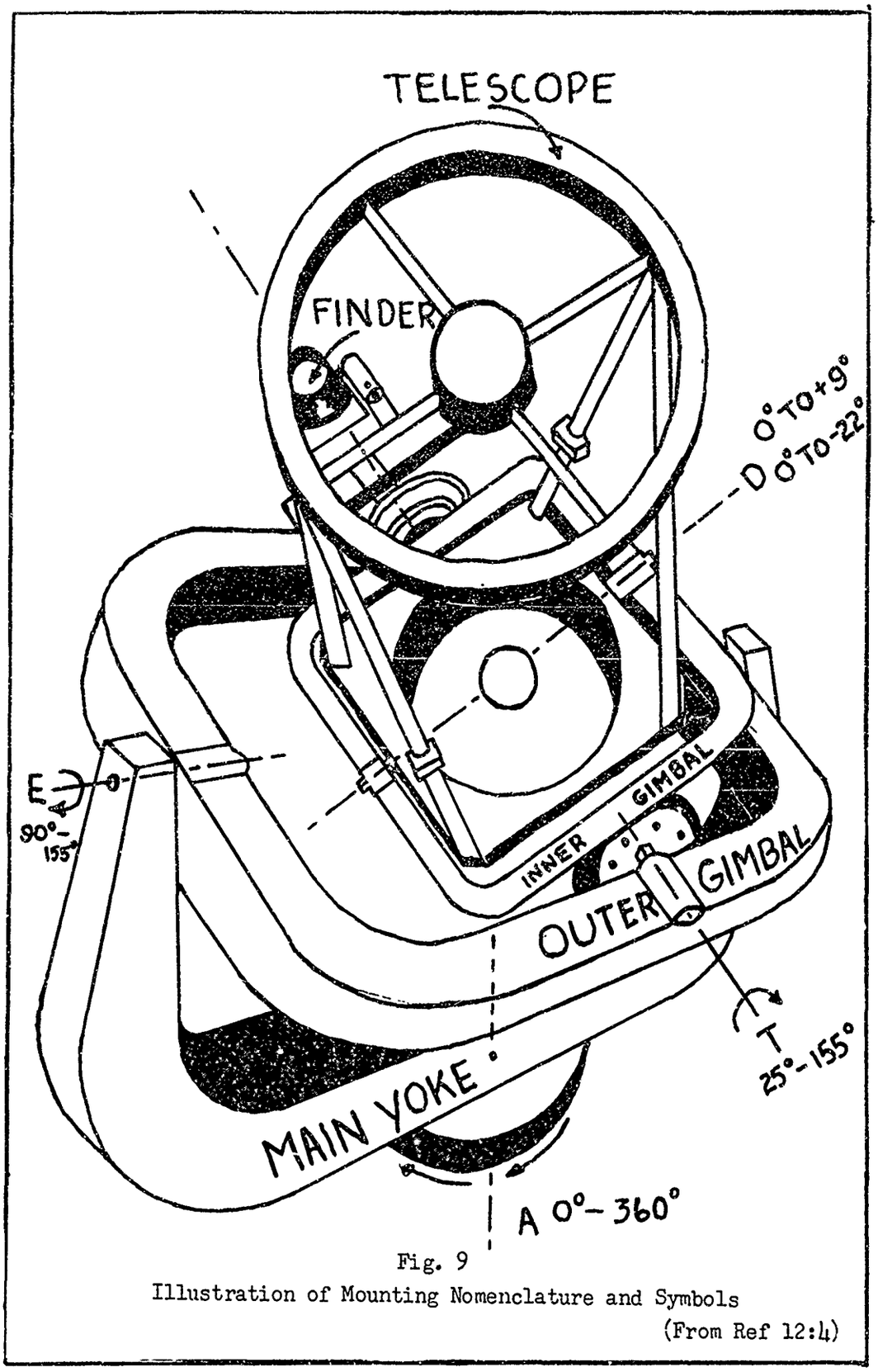

Fig. 9
Illustration of Mounting Nomenclature and Symbols
(From Ref 12:4)

as one-time fixed settings are the usual case for each satellite transit. Motion about the E axis (outer gimbal rotation) is by two means: a dc motor through a gear reduction is used for initial settings, and a selsyn system coupled to the dc motor's armature is used for vernier adjustment during tracking. Travel is free to all useful setting positions. Motion about the T axis is also accomplished by two means, where a variable speed Graham Drive is coupled through a variable-friction brake. Initial settings are made by manual slewing of the inner gimbal and telescope against brake friction; tracking is accomplished by actuation of the Graham Drive motor and continuous manual variation of the drive speed, as required by changes in satellite angular velocity. Total tracking range is about 130° (65° each side of the midpoint). Motion about the D axis is currently accomplished by manual turning of the telescope, with locking in place for fixed settings made by clamping one of the bearings. A modification is anticipated to make control of the D axis similar to that of the E axis, allowing for motorized setting, and continuous selsyn adjustment during tracking. Range is about 10° 'north' and 22° 'south'.

Polarization Analyzer

The polarization analyzer is the polarization device designed by the author for mounting on the telescope. Figure 10 shows the analyzer on and off the telescope. Figure 11 is a schematic representation of the device. Simply, it is a mechanical means of rotating a plane sheet of HN-32 Polaroid in the optical path of the light signal from the space object before its detection by the photomultiplier.

The device consists of a ball bearing of inside race diameter of approximately 4¼ inches and an outside race diameter of about 4¾ inches. The inside race of this bearing is fitted over a collar on an aluminum plate $^{3}/_{16}$ of an inch thick. This plate has a circular hole of about 4 inches in diameter drilled in it to allow a clear path through the plate and the inside diameter (plus collar width) of

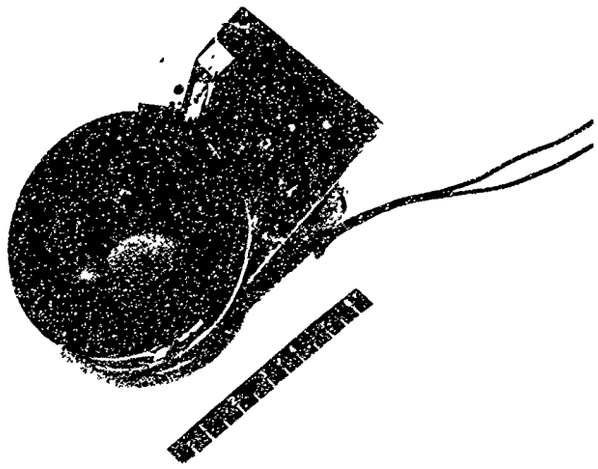

a. Off the Telescope

b. Mounted on the Telescope

Fig. 10

Polarization Analyzer

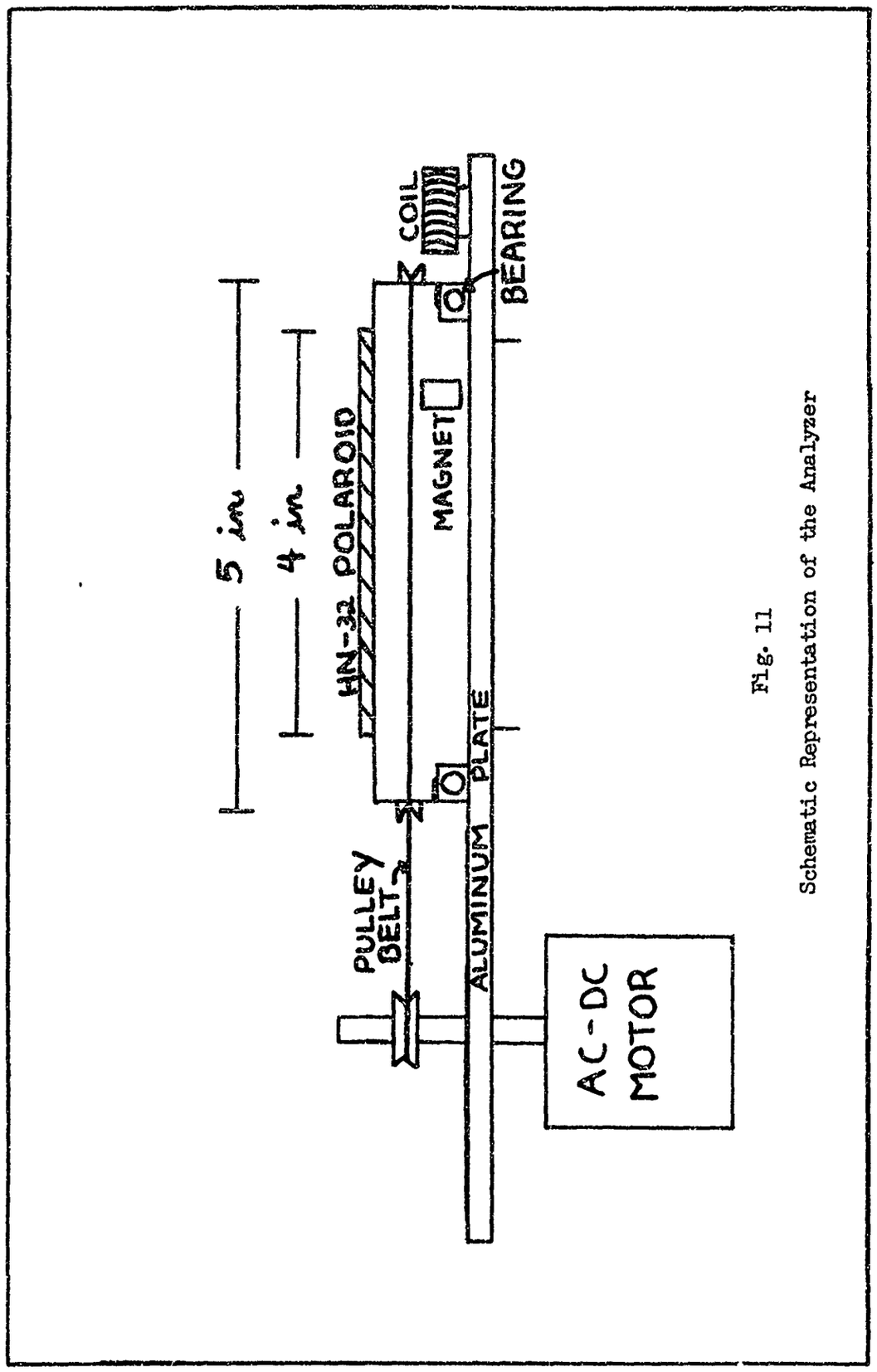

Fig. 11

Schematic Representation of the Analyzer

the bearing. Riding on the outside race, is an aluminum "can" which also has a 4 inch circular hole in it. There is, therefore, a clear path through the aluminum "can", bearing, and plate. It is over this circular hole in the aluminum "can" that the plane sheet of HN-32 Polaroid is placed. There is a groove on the outside of the "can" (outside diameter of 5 inches) which permits rotation of the "can" (and, therefore, the Polaroid sheet) by means of pulley belt and a driving motor. A ½ inch pulley is mounted on a 5000 rpm AC-DC motor which is attached to the aluminum plate. The maximum rotation rate is about 11 rps and is in a counter-clockwise direction looking down on the top of the analyzer. Also, there is a bar magnet which is mounted on the side of the aluminum "can" and a coil which is mounted on the aluminum plate near the "can". As the "can" rotates the field lines from the magnet cause a current to be induced in the coil. This current is recorded on the tape recorder and the Visicorder simultaneously. The magnet, Polaroid sheet, and coil are positioned so that when a current pulse is received the Polaroid sheet is oriented to allow passage of vertically polarized light (polarized perpendicular to the plane of incidence). This arrangement serves as a reference for the overall system. Since the coil is at an angle of 45° with the mount meridian as mentioned earlier, the plane of polarization can be uniquely determined with respect to the telescope.

The entire device is then mounted with set screws on the "stovepipe" which projects through the 24-inch mirror of the telescope. Therefore, the light, as it is focused by the secondary mirror to pass through this "stovepipe" to the photomultiplier for detection,

is modulated by the rotating analyzer on top of the "stovepipe". If polarization is present the photomultiplier sees an alternating lightening and darkening which depends on the rotational position of the analyzer.

IV. Collection of Data

Acquisition and tracking of a space object are both manual and visual. The amount is positioned to predetermined angles at a favorable point along the projected trajectory. The major requirement in finding the "predetermined angles" is the conversion of "look-angles" (local altitude and azimuth) into four-axis settings for the telescope. Look-angles, for the most part, have been provided by the USAF Air Defense Command. These are airmailed weekly in the format of the SPADATS OBSERV program, although other sources are available. The nature of the computations is such that analogue techniques work well.

The analogue device used consists of a meridional net of an equal area projection, with centrally pivoting translucent overlays. Net divisions at one degree intervals allow measuring tolerances between 0.1° and 0.2°. The circumference of the net is marked in degrees, increasing in a clockwise direction from the top, 0 - 360. Other scales denoting great and small circle intervals are needed also. The reader can find a detailed discussion with examples of this analogue technique in Vanderburgh's work (Ref 12:9-21).

The initial mount preparation is as described above. The azimuth is set, and the mount locked. Elevation is set to the predicted value; declination is set and locked, the instrument slewed to the desired acquisition track angle, and the predicted acquisition angular velocity set on the Graham Drive (initial expected tracking rate).

After the space object moves into the 6-degree finder field and is detected by the observer, the image is centered in the field by

turning on the Graham Drive motor and manipulating the elevation axis selsyn control (a fine control for movement across or perpendicular to the tracking direction). The eyepiece turret is then rotated to change the one degree field and the recording equipment turned on. Image centering is controlled by varying the tracking rate (Graham Drive) and adjusting the elevation setting. Acceptance of the target by the photometer is indicated by an audio frequency tone modulated by the light intensity of the signal. Tracking is usually continued until either the space object moves into eclipse or arrives at one of the tracking axis limits. Calibration stars are then recorded and the session completed.

It should be noted that the raw data obtained during the tracking session is logarithmic. This occurs because the brightness which is measured during the experiment is in stellar magnitudes which by definition is logarithmic. It therefore becomes necessary to convert stellar magnitude to intensity. This can be accomplished in the following way. The magnitude difference is the defining equation and is given by (Ref 2:330)

$$m - n = 2.5 \log_{10} (l_n/l_s) \tag{18}$$

where m and n are apparent magnitudes and (l_n/l_s) is the ratio of apparent brightness. Apparent magnitude or brightness refers to an object's observed brightness, which depends on its actual brightness and its distance from the observer. Notice that if one now chooses some reference magnitude, such as n = 0 magnitude, Eq. (18) can then be solved for l_s which is proportional to the intensity, I. For m = 0 magnitude $l_n = 2.257 \times 10^{-7}$ lumens/foot^2 (Ref 1:6). The solution is

$$I \propto 1_s = \frac{2.257 \times 10^{-7}}{\text{antilog } (m/2.5)} \qquad (19)$$

Therefore, using values obtained from Eq. (19) and substituting them into Eq. (9), one can obtain a value for the percent polarization.

V. Analysis of Data

Space Object #893

Space object #893 is an Able Star second stage rocket which attained orbital velocity while putting a payload into orbit. It is in a polar orbit (inclination of 89°) which is nearly circular (radius of about 1050 km). On 21 November 1966 a photometric record was obtained which contained three sets of double peaks, each peak exhibiting polarization (see Figure 12(a)).

Percent Polarization. The maximum and minimum voltages for each peak were measured and their corresponding stellar magnitudes obtained from the calibration curve for that evening, Figure 13. These values were then successively substituted in Eq. (19) to obtain values for the maximum and minimum intensities which were in turn substituted in Eq. (9) to obtain the percent polarization. The following is an example of the above procedure.

From the 893 record of 21 November 1966 the maximum and minimum voltages of the B peak in set 1 are - C.86 and - 1.41 respectively. From the calibration curve the maximum and minimum magnitudes which correspond to these voltages are +2.94 and +3.87 respectively. From Eq. (19)

$$I_{max} \propto \frac{2.257 \times 10^{-7}}{\text{antilog } (2.94/2.5)} = 1.5046 \times 10^{-8} \text{ lm/ft}^2 \qquad (20)$$

$$I_{min} \propto \frac{2.257 \times 10^{-7}}{\text{antilog } (3.87/2.5)} = 0.6390 \times 10^{-8} \text{ lm/ft}^2 \qquad (21)$$

From Eq. (9)
$$\% \text{ Pol} = \frac{1.5046 - 0.6390}{1.5046 + 0.6390} \times 100 = 40\% \qquad (22)$$

Space Object # 8[illegible]
21 Nov. 1966
Peak B Analyzer Rotation Rate = 7 rps

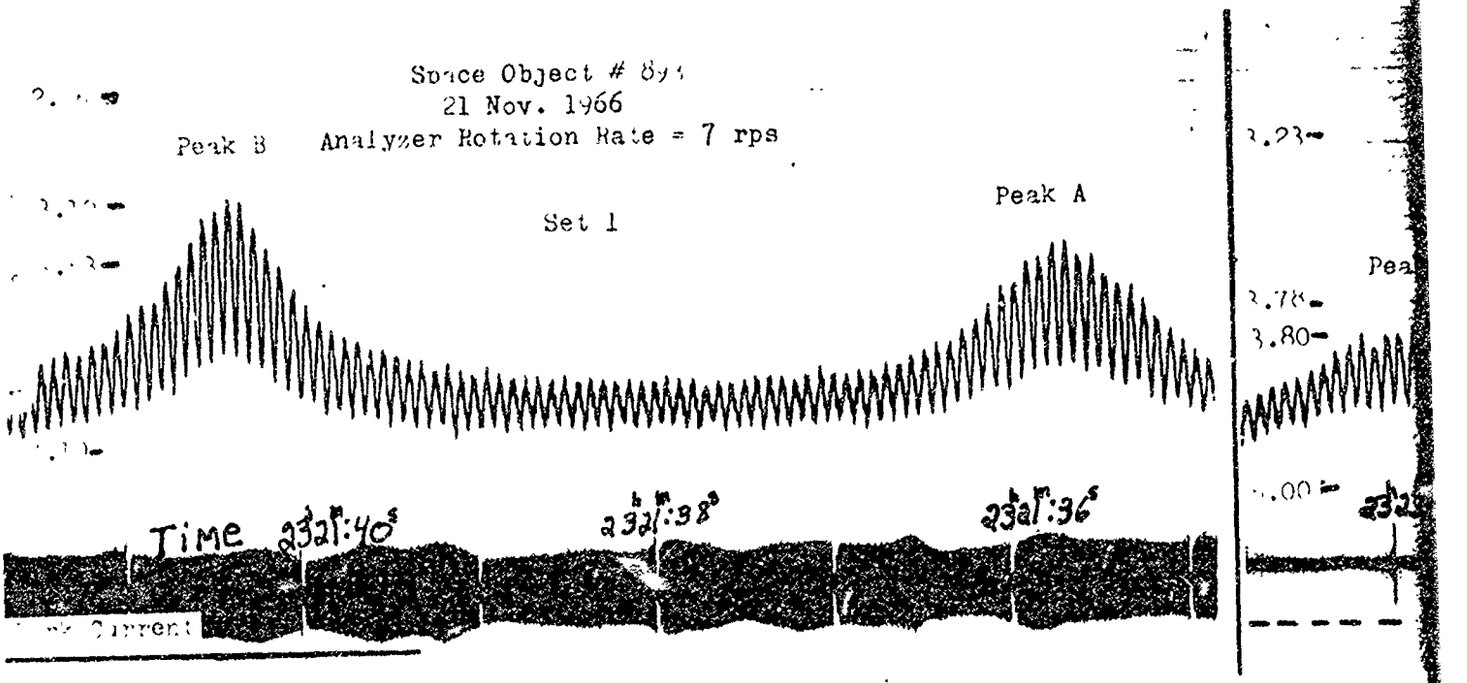

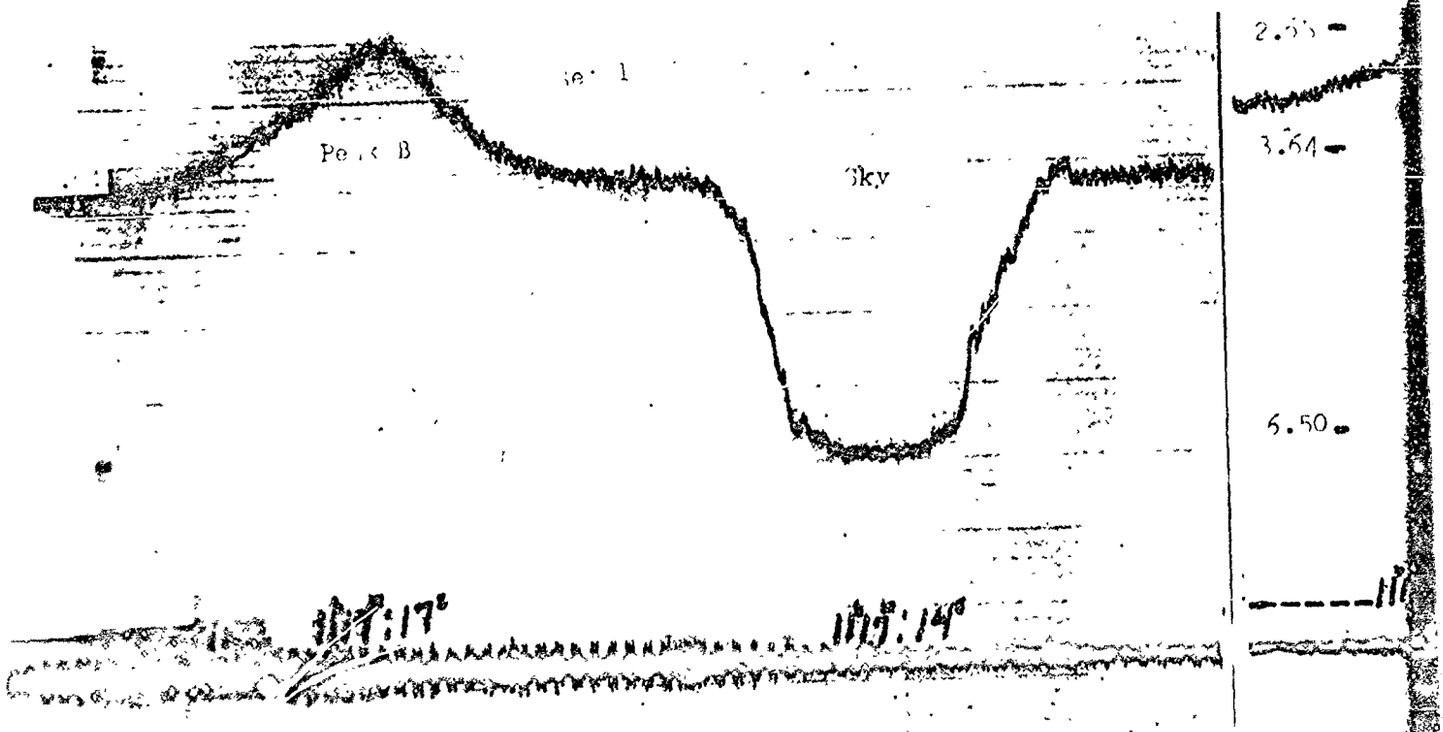

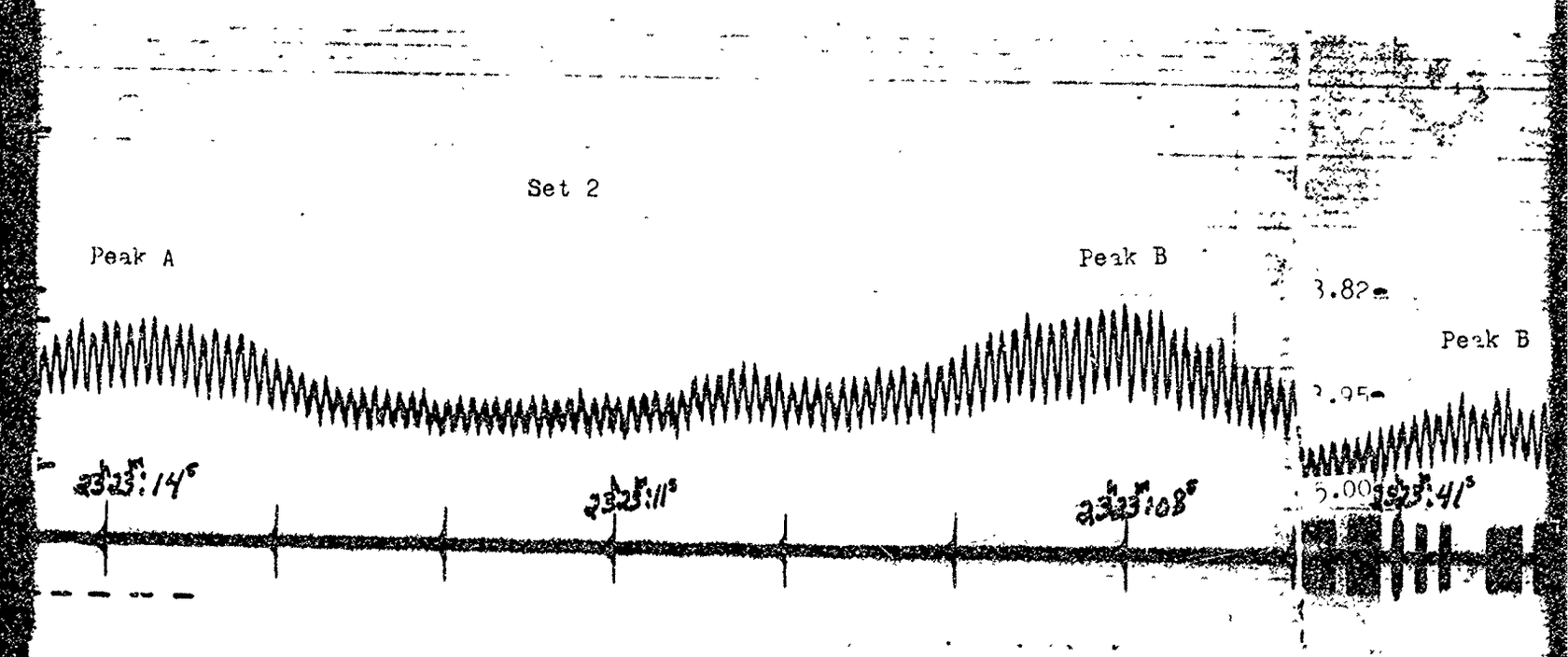

a. Space Object 893 Photometric Record with the Analyzer

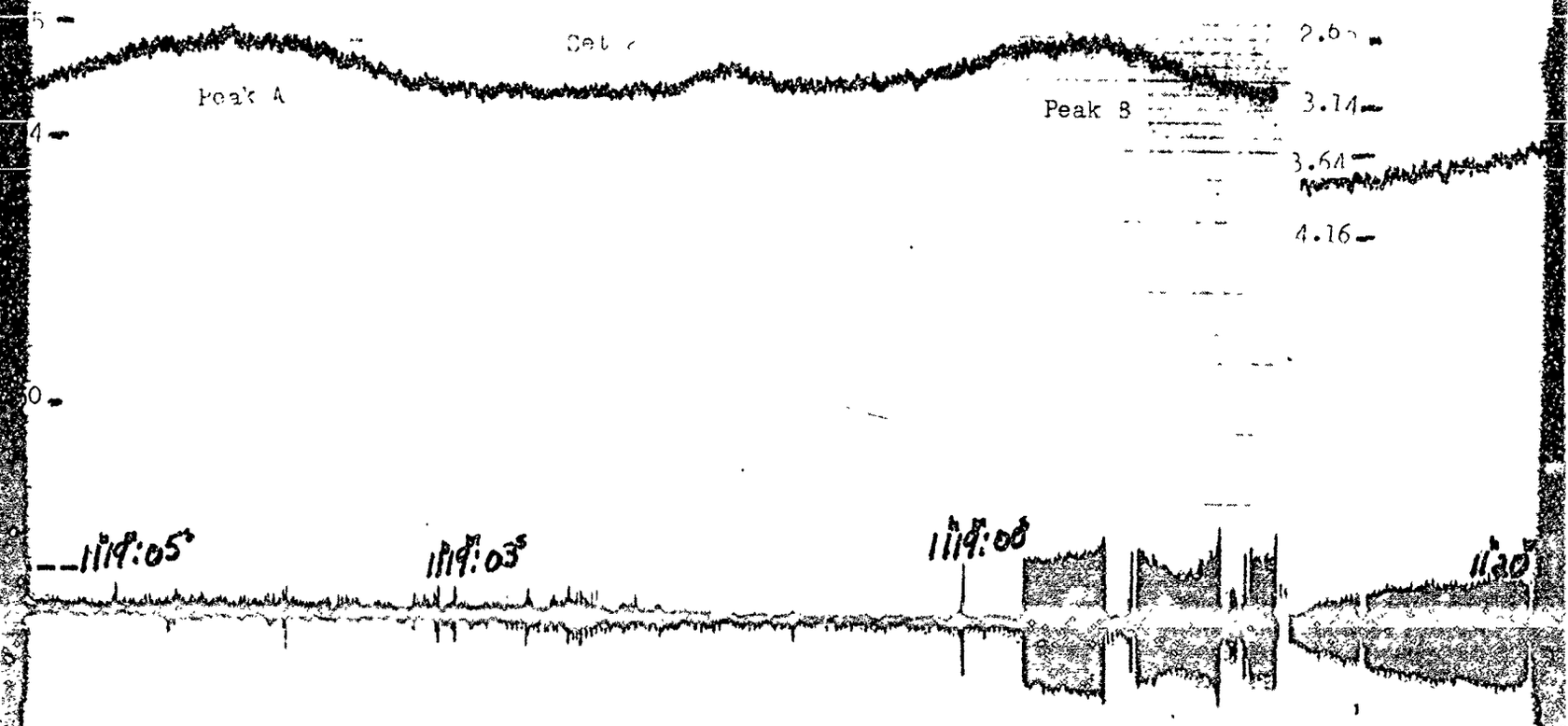

b. Space Object 893 Photometric Record without the Analyzer

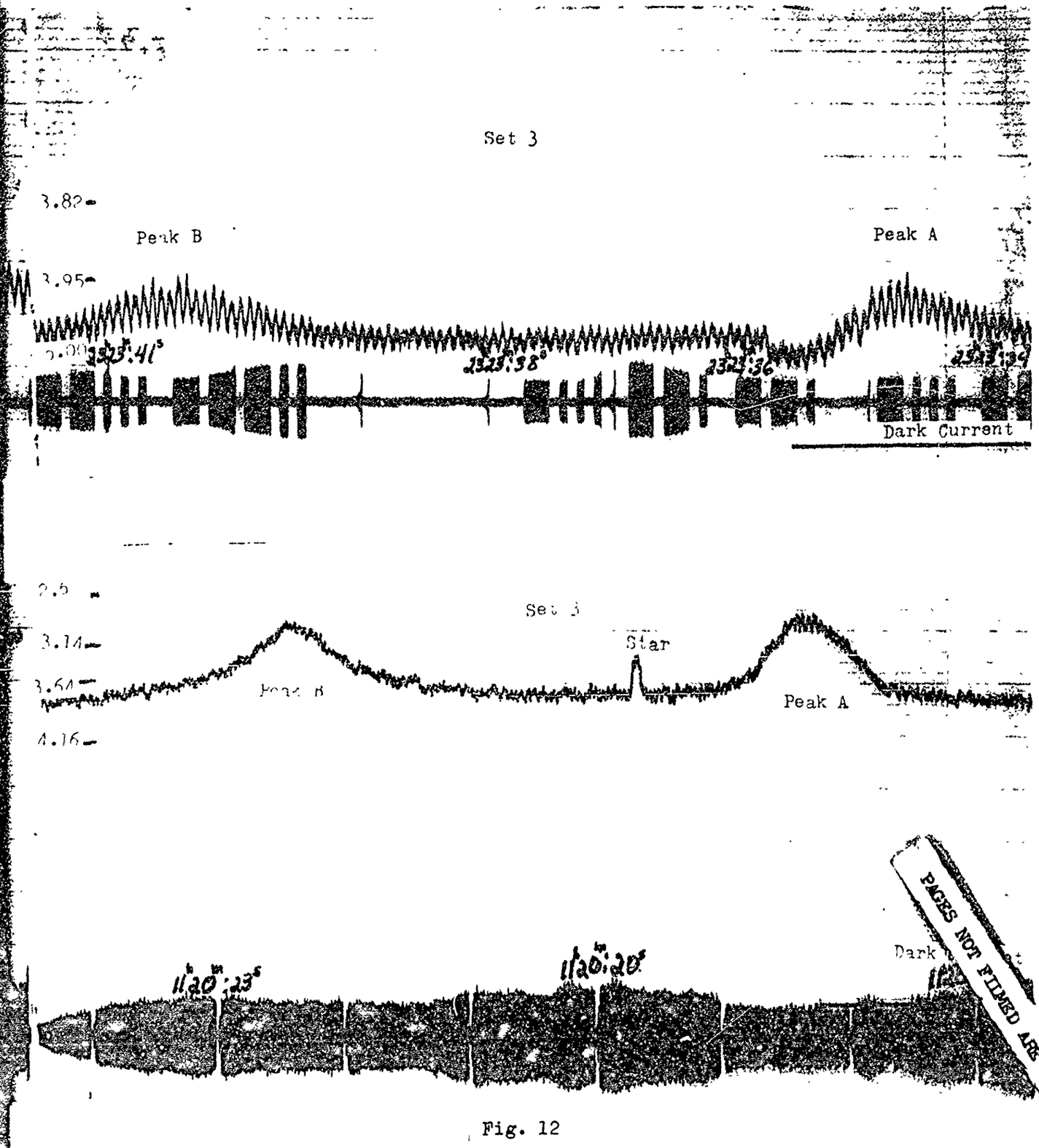

Fig. 12

Photometric Recordings of Space Object #893

3

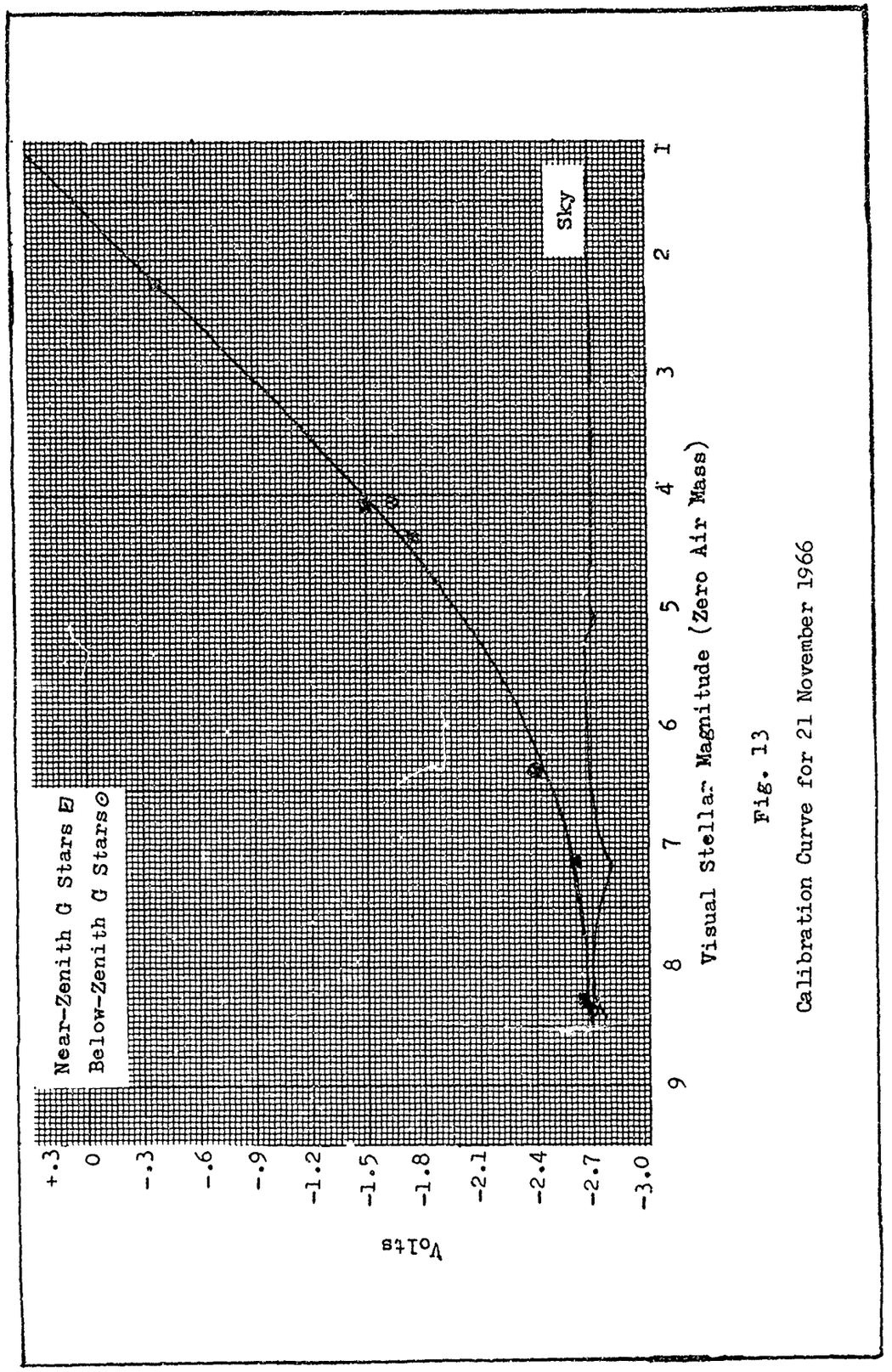

Fig. 13

Calibration Curve for 21 November 1966

In this way Table I is compiled.

Table I

Peak Polarization Percentages

Set	Time (U.T.)	Peak	%Pol
1	2321:36	A	30
	2321:40	B	40
2	2323:08	B	19
	2323:14	A	21
3	2323:35	A	20
	2323:40	B	15

In Table I the time is measured to the nearest second. Also, peaks A and B are reversed in set 2 due to rotation (i.e., order in which the "sides" are presented to the observer) of the space object.

Error Removal from the Percent Polarization. During the course of this investigation, it was discovered that the rotation of the analyzer itself introduced some modulation which was directly proportional to the intensity of the incident light. It was necessary to determine how much of this "false polarization" contributes to the "true polarization" and eliminate its contribution. Assuming that the "true polarization" does not contribute to the effect of the "false polarization," one can obtain an expression for the corrected polarization as follows. It was observed that the magnitude of the false signal was directly proportional to the intensity of the light being detected (i.e., $J = KI$).

$$I_{max} = S + D + K(S+D) = (S+D)(K+1) \tag{23}$$

and

$$I_{min} = S + D \tag{24}$$

where S is the light contributed by the sky, D is the diffuse light

from the object of interest, and K is the constant of proportionality as mentioned above. I_{max} is made up of contributions from the sky, diffuse reflection, and false signal (no polarized light is present). I_{min} is just made up of contributions from the sky and diffuse reflection since the false signal does not contribute anything to the minimum intensity. Dividing Eq. (23) by Eq. (24) defines K.

$$K = \frac{I_{max}}{I_{min}} - 1 \tag{25}$$

The value of K was determined to be 0.057.

Substituting Eqs. (23 and (24) in Eq. (9) gives

$$P_{false} = \frac{P + (S+D)(1+K) - (S+D)}{(S+D)(1+K) + P + (S+D)} \tag{26}$$

where P is the "true polarization", and the other terms are as defined before. Neglecting S (since it is accounted for by the calibration curve of Figure 13) and solving for D, one obtains

$$D = \left(\frac{1-P'}{(2+K)P' - K}\right) P \tag{27}$$

where $P' = P_{false}$.

The corrected percent polarization is given by Eq. (9) with no contribution from the false signal

$$P_{corr} = \frac{(D+P) - D}{2D + P} = \frac{P}{2D + P} \tag{28}$$

where S was neglected again for the same reason as before. Substituting Eq. (27) in Eq. (28) gives

$$P_{corr} = \frac{1}{2\left(\frac{1-P'}{(2+K)P' - K}\right) + 1} \tag{29}$$

Therefore, it is now possible to determine the "true polarization". For example, for $P' = .40$

$$P_{corr} = \frac{1}{2\left(\frac{1 - .4}{(2 + .057).4 - .0}\right) + 1} = .39$$

In this way a corrected table of percent polarization for each of the peaks on the 893 record may be compiled (see Table II below).

Table II

Corrected Peak Polarization Percentages

Set	Time (U.T.)	Peak	% P_{corr} ± 5%
1	2321:36	A	28.5
	2321:40	B	39.0
2	2323:08	B	17.0
	2323:14	A	19.0
3	2323:35	A	18.0
	2323:40	B	12.9

Variation of Percent Polarization with the Phase Angle. In the models considered earlier a plane surface was taken as a good approximation to the actual reflecting surface element, and for a specular reflector the angle of incidence and the angle of reflection were equal to each other and also to half the phase angle. This in turn defined the polarizing angle. For this transit the phase angle was a maximum when acquisition was made and continually decreased in time as the space object moved across the sky. This was true because the space object was coming from the general direction where the sun had set. If the space object had been coming from the same direction, but instead of

setting, the sun was rising, then just the opposite would have been true (i.e., increasing phase angle). The phase angles of the various peaks were measured using the analogue technique mentioned earlier. The results are listed in Table III.

Table III

Polarization Dependence on Phase Angle

Set	Peak	Phase Angle	Angle of Incidence	% Pol ± 5%
1	A	88.2	44.10	28.5
	B	87.7	43.85	39.0
2	B	82.7	41.35	17.0
	A	82.0	41.00	19.0
3	A	80.2	40.10	18.0
	B	78.7	39.85	12.9

Note that for a particular peak (A or B) the percent polarization decreases with decreasing phase angle. This is what one would expect since the angle of incidence is moving away from the maximum polarizing angle.

Absolute Magnitude of a Space Object. In order to eliminate any variation in the light signal due to range changes, a range correction is applied to bring the data in or out to a standard 1000 km. reference. This will enable the peaks which occur at different points along the orbit to be compared with each other. One would expect a nearly constant brightness for a particular peak (if referenced to a standard distance) no matter where the peak occurs along the orbit. It will also enable the verification of the result arrived at from Table III, namely, that the percent polarization decreases because the angle of incidence decreases. This will be established if the

magnitude remains nearly constant at a standard distance since a decrease in polarization implies a decrease in the change of magnitude. Therefore, if the percent polarization decreases and the magnitude remains constant, the decrease is due to a change in the angle of incidence.

Referencing to a standard distance (1000 km.) is accomplished by using Eq. (18) and the fact that the brightness is inversely proportional to the distance squared,

$$M = m - 5 \log\left(\frac{R}{1000}\right)^2 \qquad (30)$$

where M is the absolute magnitude, m is the apparent magnitude, and R is the distance of the space object. The results then obtained for the peaks of Space Object 893 are listed below in Table IV.

Table IV

Absolute Magnitudes of the Peaks

Set	Peak	Range (km.)	Apparent Mag.	Absolute Mag.
1	B	919	2.94	3.12
	A		3.35	3.53
2	A	1121	4.05	3.80
	B		4.03	3.78
3	B	1432	4.73	3.95
	A		4.75	3.97

Note that there is a slight decrease in magnitude (0.83 for A and 0.42 for B) with decreasing phase angle. However, this is most probably due to the fact that the contribution due to any diffusely reflected light decreases with phase angle (i.e., when backlit). Therefore, the magnitude of the polarizing (specular) surface is essentially a constant. Thus, the decrease in percent polarization is due to a

decrease in the angle of incidence. This is as expected from polarization theory.

Probable Value for the Index of Refraction. If a plot is made of the percent polarization versus the angle of incidence for both theoretically predicted and experimentally determined values of the percent polarization, an interesting result is obtained (see Figure 14). The Fresnel equations, Eqs. (1) and (2), predict a higher percent polarization than was observed experimentally. An index of refraction of n was used with the Fresnel equations in order to obtain the plot in Figure 14. Therefore, this is only an estimate of what percentage of polarization should have been observed since the index of refraction of the reflecting surface is unknown. However, this estimate is good enough to indicate that more polarization should have been observed.

The reason for this "contradiction" is that the Fresnel equations apply only to specularly reflecting surfaces. The space object is a specular and a diffuse reflector. It is this diffuse portion of the reflected light (when it "mixes" with the polarized light from the specular portion) that reduces the percent polarization. This can be expressed as follows.

$$I_{max} = I'_{max} + I_d \tag{31}$$

$$I_{min} = I'_{min} + I_d \tag{32}$$

where I_{max} and I_{min} are the observed maximum and minimum intensities, I'_{max} and I'_{min} are the maximum and minimum intensities respectively of the polarized portion of the light signal, and I_d is the contribution due to the diffuse reflector. From Eq. (9) it follows that

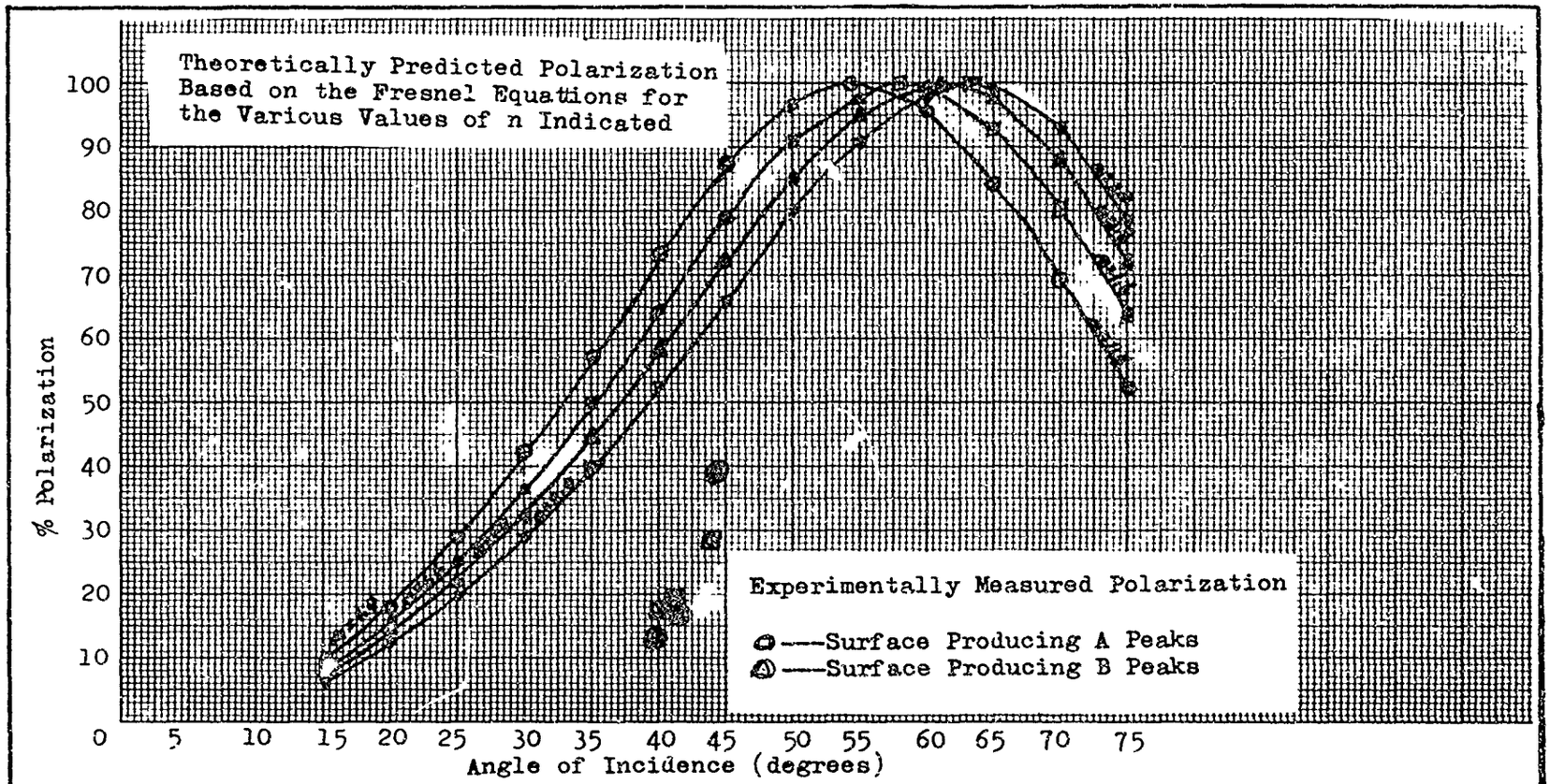

Fig. 14

Percent Polarization versus Angle of Incidence

$$P_t = \frac{I'_{max} - I'_{min}}{I'_{max} + I'_{min}} = \frac{I'_{max} - I'_{min}}{I_{max} + I_{min} - 2I_d} \tag{33}$$

and

$$P_o = \frac{I'_{max} - I'_{min}}{I'_{max} + I'_{min} + 2I_d} = \frac{I'_{max} - I'_{min}}{I_{max} + I_{min}} \tag{34}$$

where P_t = polarization due to specularly reflecting, dielectric surfaces and P_o is the observed polarization due to effect of the diffusely reflected light.

Therefore,

$$\frac{P_t}{P_o} = \frac{I_{max} + I_{min}}{I_{max} + I_{min} - 2I_d} \tag{35}$$

In order to obtain a value for P_t it is necessary to obtain a value for I_d. However, I_d cannot be determined since neither it nor I'_{max} or I'_{min} were measured directly in the experiment. An attempt was made to find I_d from Eq.(35) by assuming a value for P_t and by using the measured R for the angle of incidence of interest. The I_d thus found was plugged back into Eq.(35) for different angles of incidence (corresponding to different P_t) to see whether the P_t thus calculated fit or converged to one of the family of curves in Figure 14. However, the results were negative so that no definite value for the index of refraction could be found.

However, measurements were made in the lab to determine the polarizing angles for some glossy paints since this was the type of dielectric surface believed to have produced the polarization (see Figures 12 and 16). The results of these measurements are listed in Table V below. These measurements were made by shining light on the glossy painted surfaces and using a plane sheet of HN-32 Polaroid to measure the reflected angle at which maximum

polarization occurred.

Table V

Polarizing Angles for Glossy Paints

Paint	Type of Surface	Polarizing Angle ± 2°
Acrylic Lacquer	glossy	57°
Yellow	semi-glossy	60°
Gray	semi-glossy	66°
Gray	glossy	61°

Plane of Polarization. From the theoretical development it was determined that the electric vector should vibrate perpendicular to the plane of incidence (phase plane). Unfortunately no analyzer marker was recorded for the 893 record on 21 November 1966. However, another successful record on a different object, Space Object 426, was taken on 10 February 1967 by Mr. Vanderburgh (see Figure 15). Excellent analyzer markers and moderately strong polarization were recorded. The use of another space object should make no difference in the outcome since all that is being determined is the position of the electric vector with respect to the plane of incidence. It follows from Eqs. (16) and (17) that

$$\sin a = \frac{\sin TA \sin EL_t}{\sin (90 - EL_s)} = \frac{\sin (22.6) \sin (29.0)}{\sin 63.2} = .20873 \qquad (36)$$

and

$$\sin B = \frac{\sin A \sin (90 - EL_{sun})}{\sin \phi} \qquad (37)$$

$$= \frac{\sin (181.2) \sin (64.8)}{\sin 138} = .02839$$

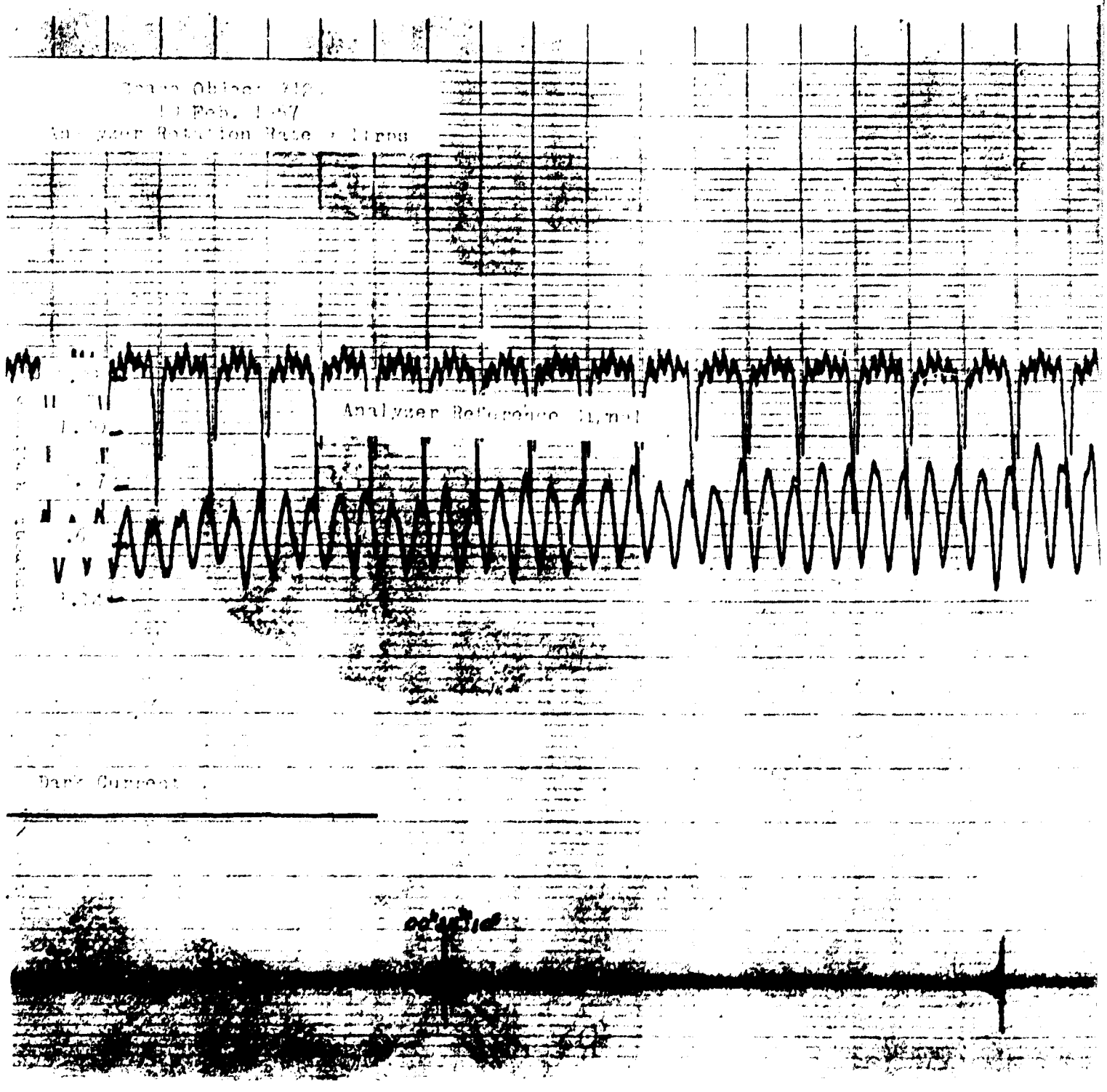

Best Available Copy

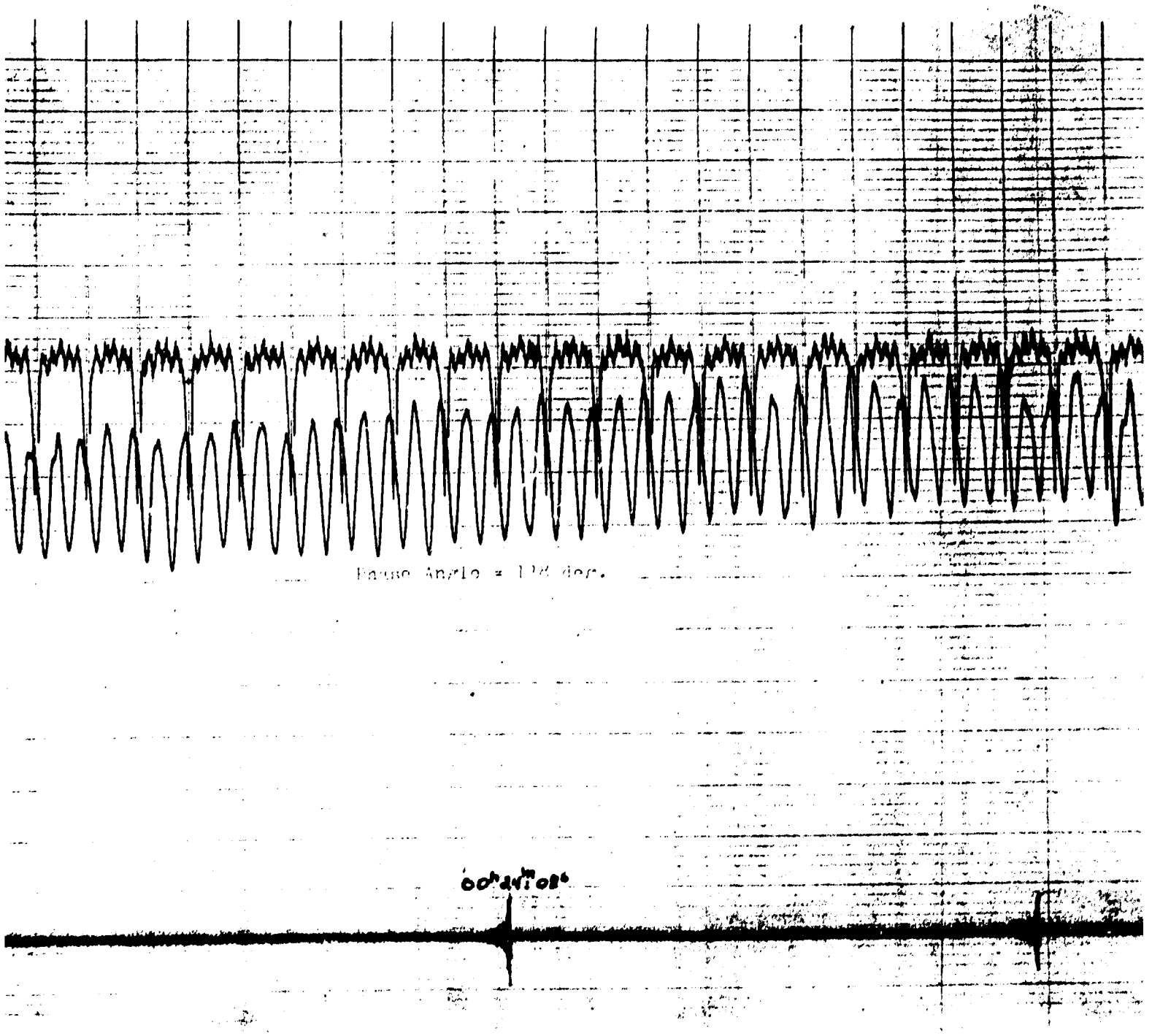

2

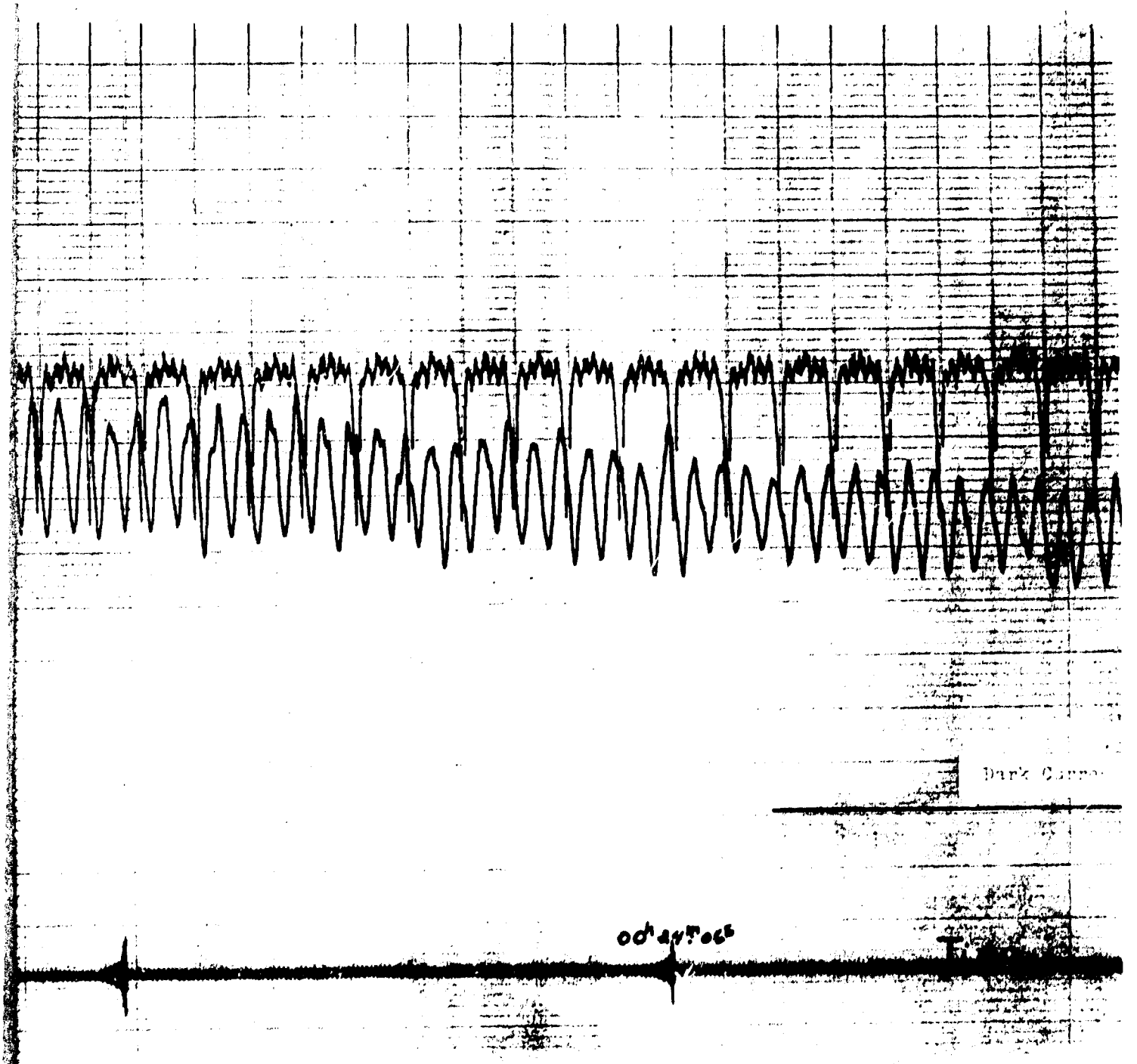

Fig. 11

Photometric Recording of Space Object #426

3

where TA and EL_t are determined from the mount settings, and EL_s, A, Ø, and EL_{sun} are determined using the analogue technique mentioned earlier with values for the sun's position taken from The Air Almanac (Ref 10:650). Therefore, "a" is equal to 12° and B is equal to 1.6°. Since B is less than "a" the quantities add to give

$$b = 13.6° \tag{38}$$

where b is the angle between the phase plane and the mount meridian.

By direct measurement from the analyzer marker on the record, Figure 15, a maximum for vertically polarized light (perpendicular to the plane of incidence) occurred at 10.4° ± 10° measured clockwise from the mount meridian. The large uncertainty of 10° is due to the limitation of the FM tape recorder in playing back the reference signal of 11 cycles/sec for the expanded representation of the record. Nevertheless, the predicted and experimental results are in satisfactory agreement.

Comparison with an Unpolarized Record. It is of some value to compare the record of Space Object 893 which exhibits polarization with another record of Space Object 893 for which the analyzer was not on the telescope, Figure 12(b).

It can be seen that although the overall signature pattern is the same (i.e., three sets of double peaks), the modulation due to the detection of polarized light by the analyzer is not present. This would suggest that the modulations are not due to some repetitive motion of the object. Indeed, since the frequency of modulation for the polarized record is twice the rotational frequency of the analyzer (due to the 180° ambiguity of the Polaroid), this would indicate that

it is the light itself (polarized) which is responsible for the modulation.

Probable Explanation for Peaks. It can be seen from the records of Space Object #893 that two characteristic peaks re-occurred periodically. The fact that peaks were present is a consequence of the reflecting area "exposed" to the observer. As the space object tumbled the scattering area went from a minimum (end view for a cylinder) to a maximum (side strip). The maximum scattering area produced the peak. The fact that there were two peaks might best be explained by assuming that the light was scattered by two separate surfaces at an angle to each other. Indeed, if one looks at a photograph of this type of rocket (See Figure16), one sees that the tail section is flanged out from the front section. However, no obvious relation between the conical angle and the peak separation could be found.

Space Object #1092

Space Object #1092, a Russian rocket body, was observed on 12 February 1967 and the record shown in Figure 17(a) obtained. Polarization has the best chance of occurring where the phase angle is large. The phase angle was large at the beginning of the track and decreased in time as the space object moved across the sky. The first part of the record corresponding to large phase angles was examined for polarization. No polarization could be detected.

Comparison with an Unpolarized Record. Comparing the 1092 record taken with the analyzer on, Figure 17(a), with the 1092 record of 24 September 1966, Figure 17(b), taken without the analyzer shows the

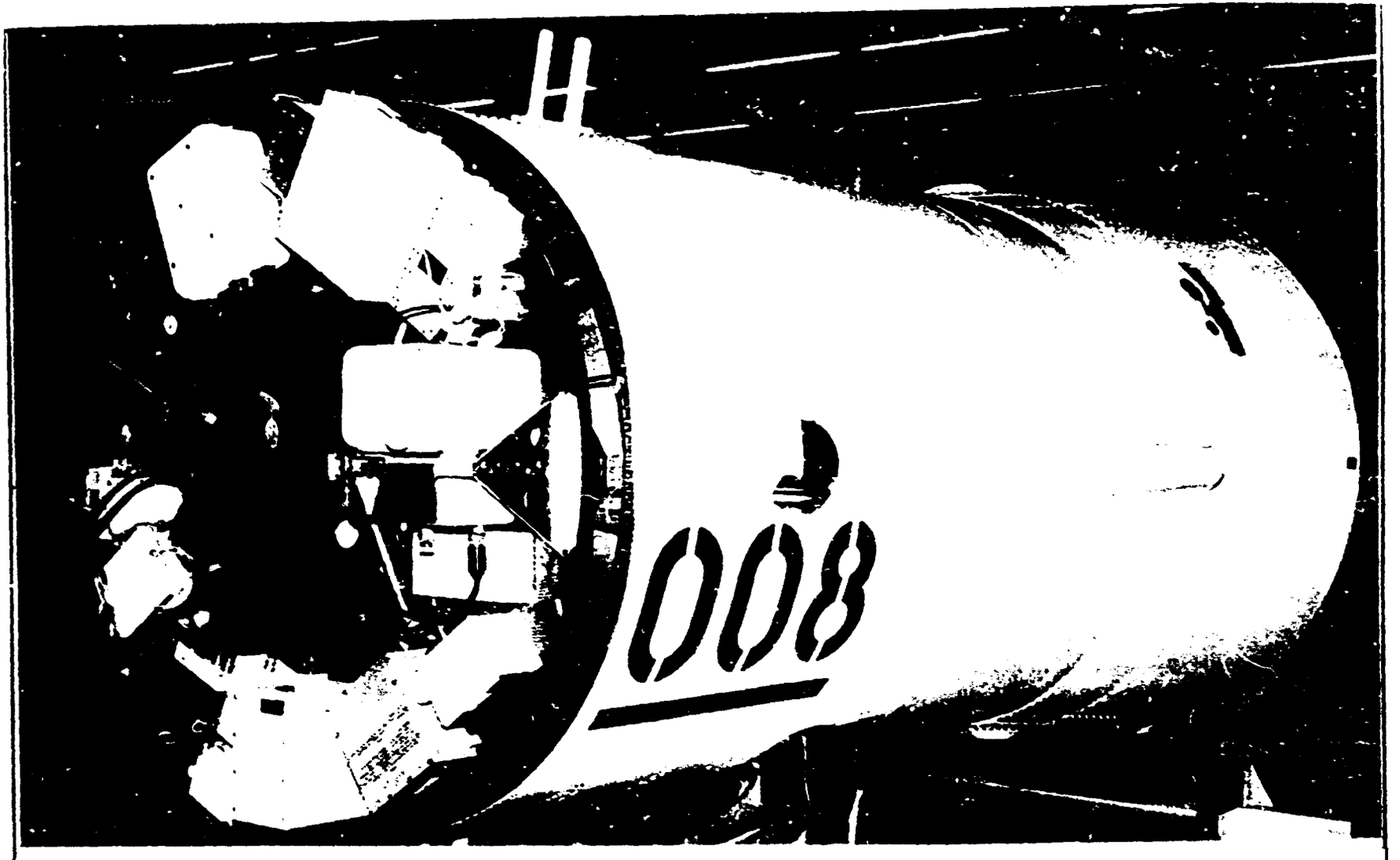

Fig. 16 Ablestar Rocket Body

The particular rocket pictured was used to launch the 1961 Omicron and is representative of the series to which Space Object #893 belongs.

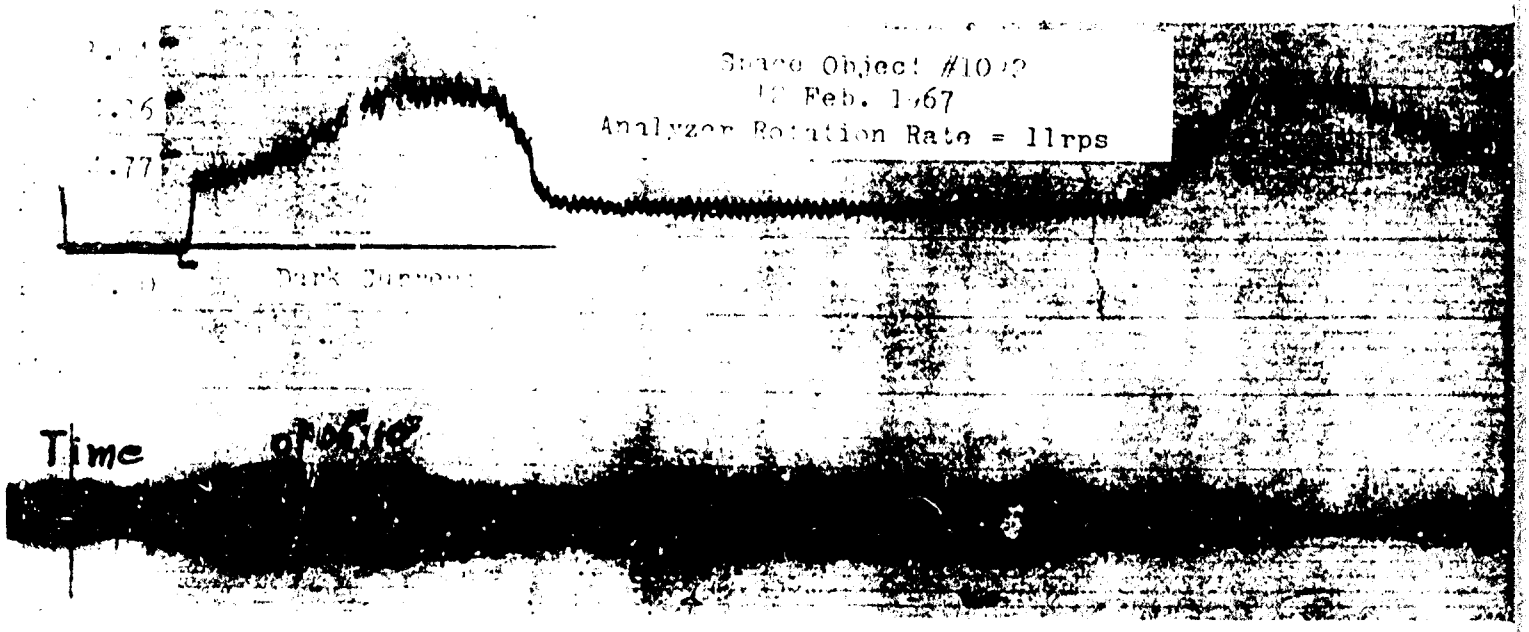

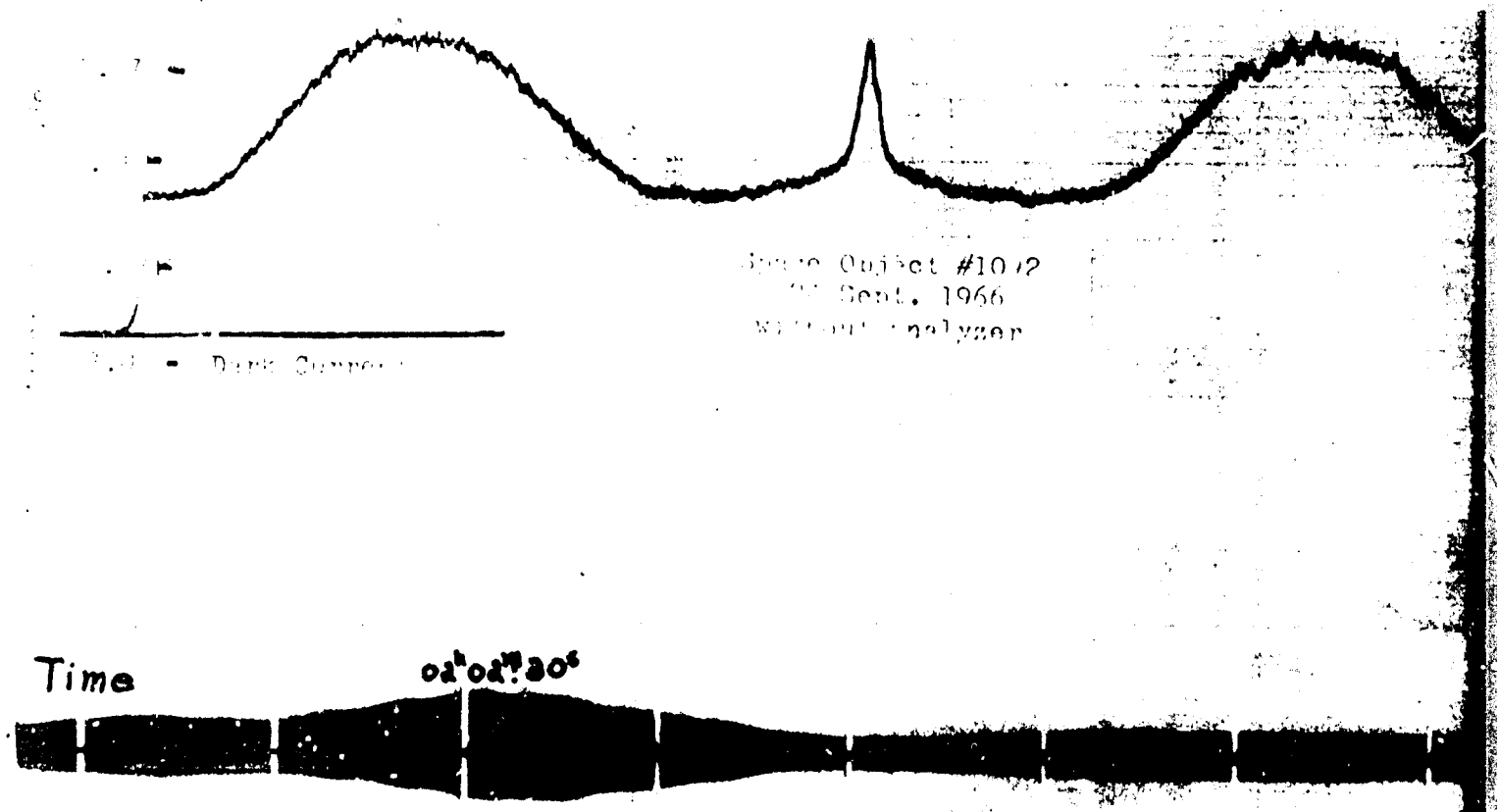

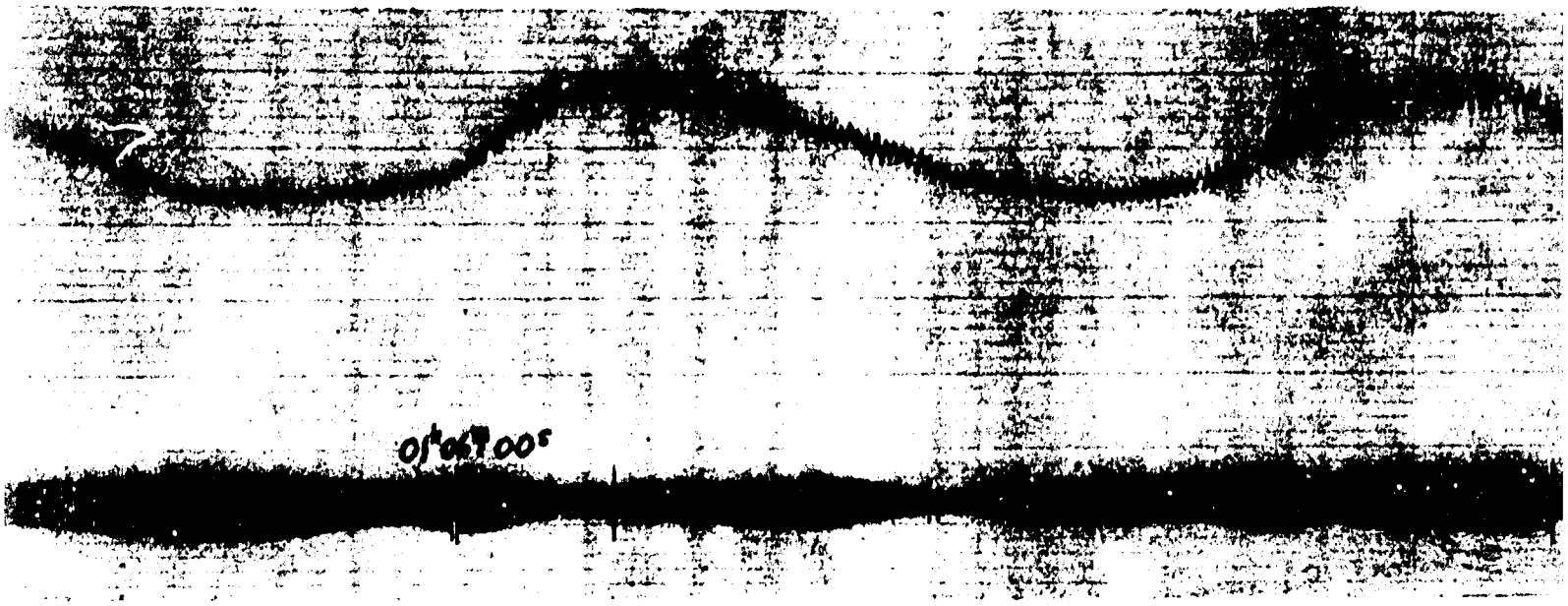

a. Space Object 1092 Photometric Record with the Analyzer

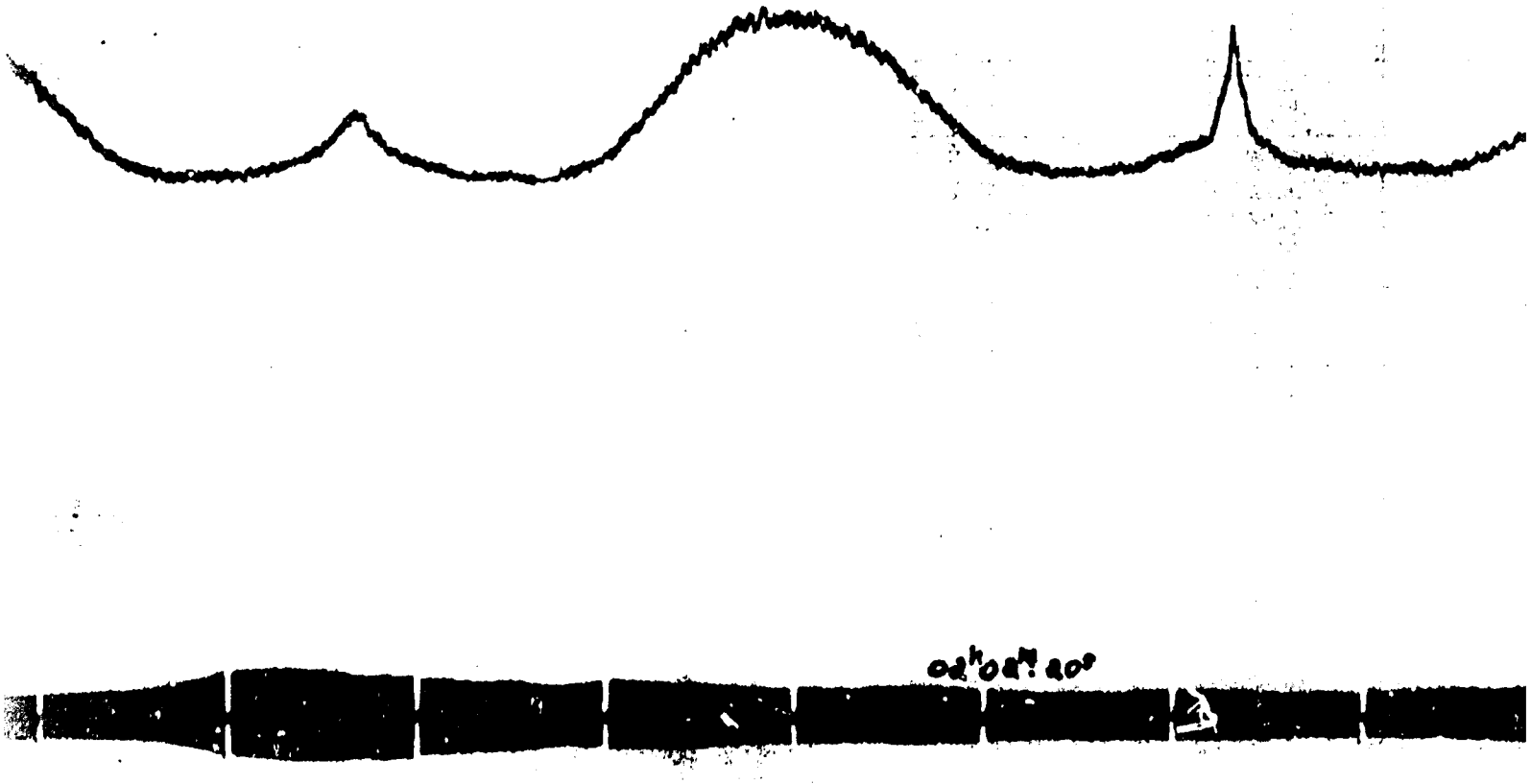

Space Object 1092 Photometric Record without the Analyzer

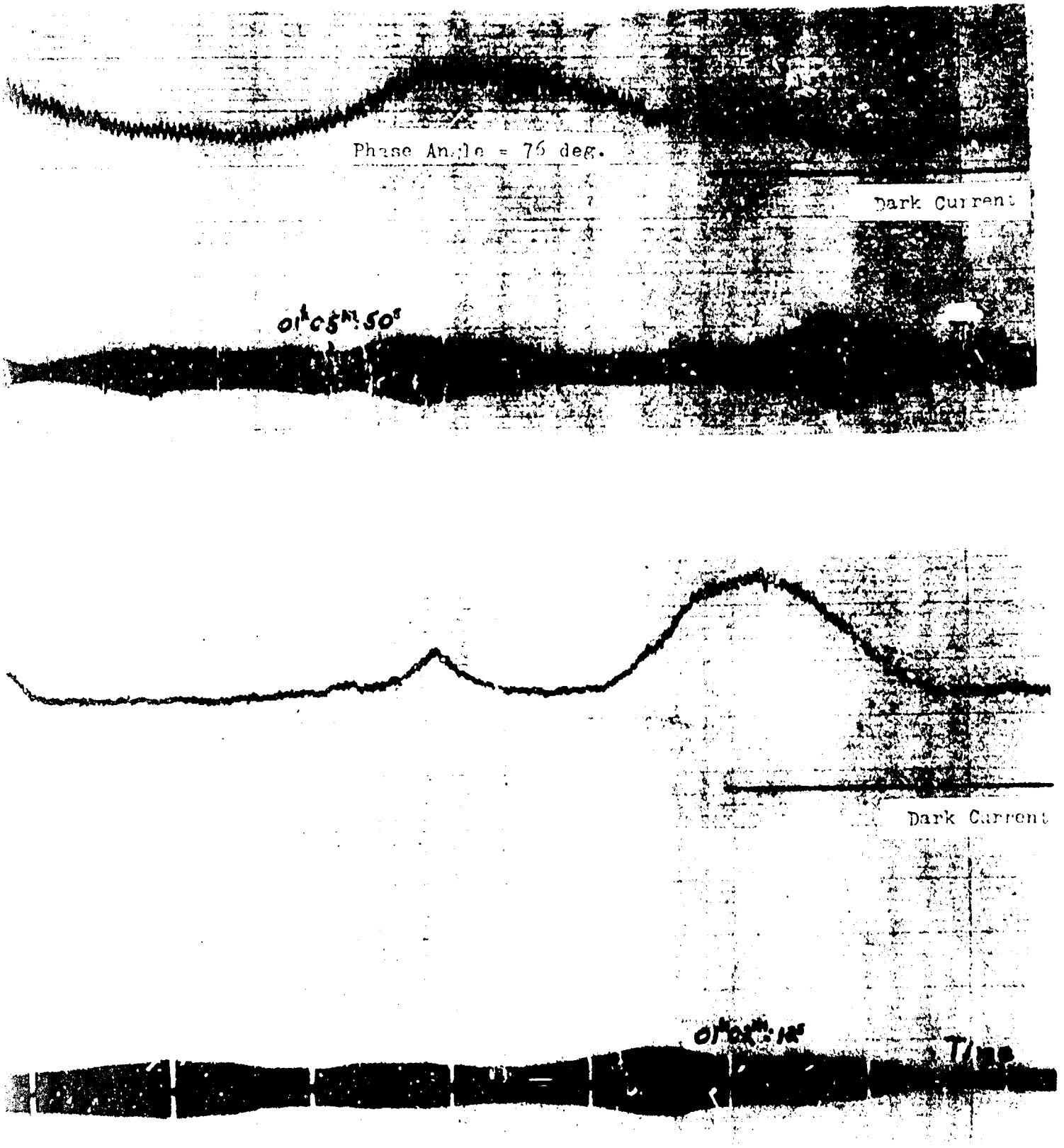

Fig. 17

Photometric Recordings of Space Object #1092

same signature pattern for both. Therefore, since both patterns are the same, there is no polarization present (since the presence of the analyzer does not matter).

Explanation for No Apparent Polarization. The most probable reason for not receiving any polarized light is that the reflecting surface is not a specular dielectric. Indeed, from the rounded nature of the peaks in Figure 17 one can state fairly confidently that the light was reflected from a diffuse surface. A glossy metal surface is ruled out since it would have produced peaks with sharp points.

VI. Conclusions and Recommendations

Conclusions

Plane polarized light scattered from a space object was observed in good accord with theoretical expectations. The theoretically predicted and experimentally measured planes of polarization were in good agreement. Also, the percent polarization tended to decrease with decreasing phase angle, in accord with theoretical expectations. These facts, when taken together, are consistent, in that in general the results predicted from the theory of polarization were observed experimentally. Therefore, it can be concluded that (1) polarization by reflection from an object in space does occur, (2) this polarization can be detected and measured by an observer on the earth, and (3) the model of the plane surface approximation, upon which the predictions were based, is a good one.

Recommendations

Only linearly polarized light was considered in this investigation. Theoretically, it is possible for a specular metal surface to produce elliptically polarized light by reflection (Ref 3:124). This should be considered as the next step in any modification of the present system. This could be done by introducing an optical retarder which could be rotated independently from the analyzer.

Also, the present analyzer should be refined and made a more permanent part of the system. This could be accomplished by reducing its size and positioning it closer to the photometer. It would then be possible to introduce a beam splitter and analyze

one beam for polarization and use the other one for phtography, color properties, or diffraction experiments. The latter two should certainly be considered as a further area for investigation.

Moreover, the addition of definite information on the object orientation as inferred from radar to the input information would be very useful. This would enable the observer to decide more accurately which part of the surface on the space object is producing the polarized light.

Finally, it is recommended that the compiling of a catalogue of the polarization properties of space objects be continued. This could be a useful aid in the classification and identification of space objects as well as a means of obtaining definite information on their surface characteristics. The latter could then be used for determining the deterioration a surface has undergone due to the space environment.

Bibliography

1. Allen, C.W. Astrophysical Quantities. New Jersey: Essential Books, 1955.

2. Baker, R.H. Astronomy. New Jersey: D. Van Nostrand Company, Inc., 1959.

3. Chorvinsky, M., et al. Optical Phenomena in Space. Technical Report 61-163. Griffiss Air Force Base, Rome, New York: Rome Air Development Center.

4. Hardy, H.C., and F.H. Perrin. The Principles of Optics. New York: McGraw-Hill Book Company, Inc., 1932.

5. Hiltner, W.A. "Polarization Measurements." Astronomical Techniques. Edited by W.A. Hiltner. Chicago: The University of Chicago Press, 1962.

6. Kissell, K.E. Advantages of a 4-Axis Tracking Mount for the Photoelectric Photometry of Space Vehicles. ARL 65-260. Wright-Patterson Air Force Base, Ohio: Aerospace Research Laboratories, 1965.

7. Kissell, K.E. Photoelectric Photometry - A New Tool for Satellite Signatures. Proceedings of the O.A.R. Washington: Office of Aerospace Research, 1966.

8. Menzel, D.H. Our Sun. Cambridge: Harvard University Press, 1959.

9. Stiles, G.J. Prediction of Apparent Magnitude of Distant Missiles in Sunlight. Memorandum Report No. 10008. Aberdeen Proving Ground, Maryland: Ballistic Research Laboratories, 1956.

10. United States Naval Observatory. The Air Almanac. May-August 1966. Washington, D.C.: Department of the Navy, 1965.

11. Vallerie, E.M., III. Investigation of Photometric Data Received from an Artificial Earth Satellite. Thesis. Wright-Patterson Air Force Base, Ohio: Air Force Institute of Technology, 1963.

12. Vanderburgh, R.C. A Prediction and Tracking Method for Small-Aperture, Continuous Optical Tracking of Artificial Satellites. ARL 66-0008. Wright-Patterson Air Force Base, Ohio: Aerospace Research Laboratories, 1966.

13. Zirker, J.B., F.L. Whipple and R.J. Davies. "Time Available for the Optical Observation of an Earth Satellite." Scientific Uses of Earth Satellites. Edited by James Van Allen. Ann Arbor: The University of Michigan Press, 1956.

Appendix A

Four-Axis Geometry (Ref 12:9)

Figure 18 illustrates a local satellite trajectory passing through the points X_1, X_2, X_3. These points are first located by conventional alt-az coordinates, then fit to the best small circle SS′ whose equator is the great circle GG′, and whose pole P coincides with the mount's tracking axis T. The point X_2 happens to coincide with the midpoint of symmetry; T on the mount scale is 90° and the azimuth of this point is the A setting. D is the displacement of SS′ from GG′ in great circle degrees, and is usually "down" or "southern" (negative).

Analog solution to the "best fit" problem first requires a plot of three or more look angle (alt-az) points. The approximate midpoint of symmetry of the curve connecting the plotted points is determined by inspection (in this case X_2). Point P lies on the vertical circle through the point X_2, and is found by first estimating the value of D. The angular distance of P from X_2 is D + 90°. With P approximated, D values may be measured and marked "up" from the points X along vertical circles joining each X point with P. The correct value of D is the one for which a single great circle (an equator) joins the points X_1', X_2', X_3'. If the initial D estimate differs from a suitable value by more than a few degrees, point P is repositioned, and the procedure repeated. Once the best D value has been determined, a precise A value may be found (GG′ will fit all three X′ points only when A is correct). A good fit is considered to have been accomplished when the true D displacements of each plotted point from a common equator differ from each other by less than 0.4°, within a T range of about 130°.

Angular velocity is obtained through a simple empirical formula relating slant range to arc seconds per time seconds: 1,440,000 divided by the slant range (km). Although not precise, this method is sufficiently accurate for acquisition purposes.

4- Axis Geometry

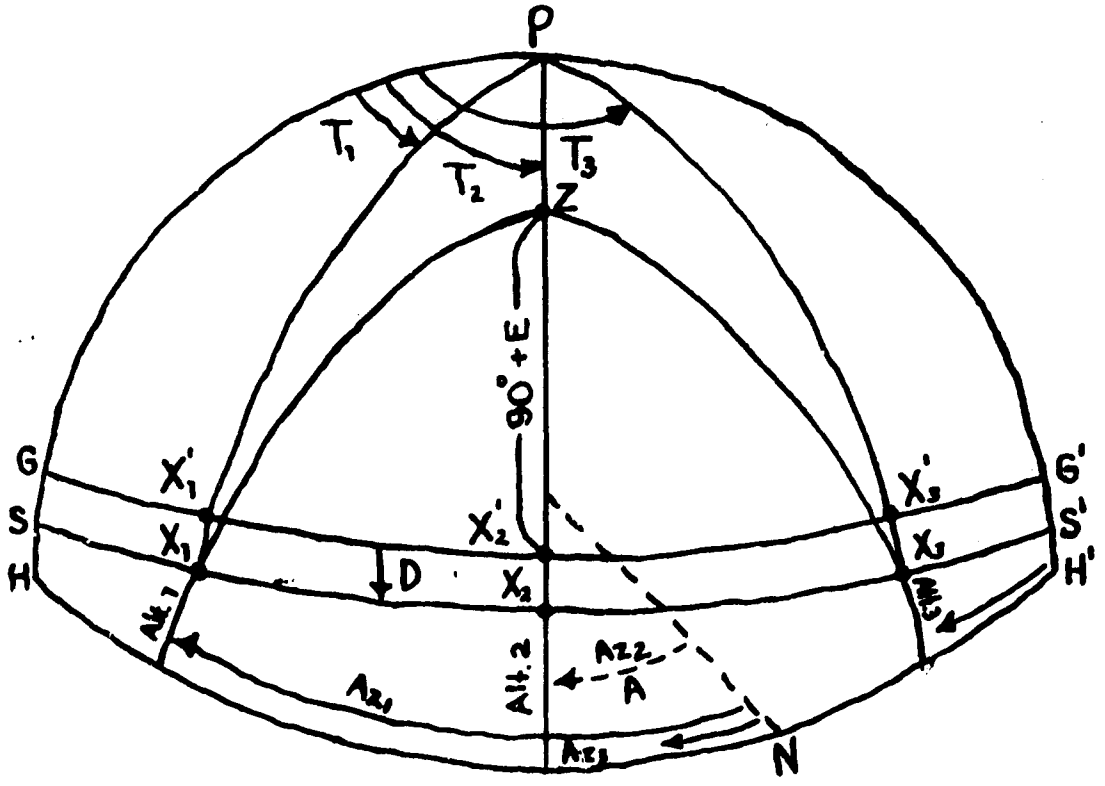

P = "Upper" pole of the T Axis

GG′ = Great circle set by E Axis

SS′ = Best fit small circle to satellite path

D = Negative when "down"

HH′ = Local Horizon

Z = Local Zenith

Alt = Altitude (Elevation) of satellite

Az = Azimuth of satellite

N = True North

Fig. 18

Celestial Sphere Representation of Local Satellite Trajectory

(From Ref 12:10)

Appendix B

Sample Calculation

The illumination E received by an observer from a plane surface object is given by Eq.(10) ,

$$E = \frac{I\omega}{A} \qquad (10)$$

where the quantities are as defined before. The shape of the area will be an ellipse due to the fact that the $\frac{1}{2}^{\circ}$ reflected light cone will intercept the surface of the earth at some angle (similar to a flashlight beam shining on a wall at an angle). The area for an ellipse is given by

$$A = \pi/4\ (ab) \qquad (39)$$

where a and b are major and minor axes respectively.

A 5 magnitude star, from Eq.(19), corresponds to 2.257×10^{-9} lm/ft^2. Therefore, the observed illumination equals 2.257×10^{-9} lm/ft^2 which in turn equals Eq.(10). In order to determine the luminous flux of the reflected beam the area in Eq.(39) must be determined.

$$b = r\,d\theta = 1000 \times 1800'/206{,}265'' = 8.726 \text{ km.}$$

a = b for an angle of incidence of 0° with the normal to the surface and becomes infinite as the angle of incidence approaches 90°. This suggests the following relationship

$$a = b/\cos i \qquad (40)$$

where i is equal to the angle of incidence. Therefore,

$$a = 8.726/\cos 60 = 17.452 \text{ km.}$$

$$A = ab = 119.72 \text{ km}^2$$

With the area now determined the luminous flux is given by

$$\text{luminous flux} = EA = 2.257 \times 10^{-9}\ \text{lm/ft}^2 \times 119.72\ \text{km}^2$$

Using the fact that $1\ \text{km}^2 = 1.0764 \times 10^7\ \text{ft}^2$, gives a luminous flux of 2.9 lm. This 2.9 lumens is the flux scattered by the "effective" area of the plane surface, i.e.,

$$2.9\ \text{lm} = 13{,}136\ \text{lm/ft}^2 \times \text{effective area ft}^2/144$$

where 144 is for the conversion to square inches and 13,136 is the solar illuminance in the vicinity of the earth. This corresponds to an area of 0.02 in^2.

UNCLASSIFIED
Security Classification

DOCUMENT CONTROL DATA - R & D

(Security classification of title, body of abstract and indexing annotation must be entered when the overall report is classified)

1. ORIGINATING ACTIVITY *(Corporate author)*
Air Force Institue of Technology (AFIT-SE)
Wright-Patterson AFB, Ohio 45433

2a. REPORT SECURITY CLASSIFICATION
UNCLASSIFIED

2b. GROUP

3. REPORT TITLE
An Investigation of Polarization Phenomena Produced by Space Objects

4. DESCRIPTIVE NOTES *(Type of report and inclusive dates)*
AFIT Thesis

5. AUTHOR(S) *(First name, middle initial, last name)*
Stead, Richard P., 1/Lt., USAF

6. REPORT DATE	7a. TOTAL NO. OF PAGES	7b. NO. OF REFS
June 1967	62	13

8a. CONTRACT OR GRANT NO. N/A	9a. ORIGINATOR'S REPORT NUMBER(S)
b. PROJECT NO. N/A	AFIT Thesis GSP/PH/67-7
c.	9b. OTHER REPORT NO(S) *(Any other numbers that may be assigned this report)* N/A
d.	

10. DISTRIBUTION STATEMENT
Distribution [redacted]

11. SUPPLEMENTARY NOTES	12. SPONSORING MILITARY ACTIVITY
	Aerospace Research Laboratories General Physics Laboratory Wright-Patterson AFB, Ohio 45433

13. ABSTRACT

Plane polarized light produced by the reflection of sunlight from a dielectric surface on a space object was observed. This was accomplished with a polarization analyzer which was added to the existing photoelectric telescope and recording equipment at the Sulphur Grove, Ohio tracking station. A maximum of 39% polarization was measured for one particular satellite (Space Object #893). The plane of polarization was found to be perpendicular to the plane of incidence as expected.

DD FORM 1 NOV 65 1473

UNCLASSIFIED

14. KEY WORDS	LINK A		LINK B		LINK C	
	ROLE	WT	ROLE	WT	ROLE	WT
Polarization Percentage						
Polarization Analyzer						
Space Objects						
Satellites						
Plane polarized light produced by reflection						
Dielectric Surfaces						
Photoelectric Telescope						
Plane of polarization						
Plane of incidence						